Regulation of polypyrimidine tract-binding protein 1- by class IA phosphoinositide 3-kinase p110β activity in cancer cells.

Ifeoluwa Abigail Oyediran

Department of Biological Sciences

Faculty of Mathematics and Natural Sciences

University of Bergen

Nov 2022

This thesis was submitted in partial fulfilment of the requirements for the degree of Master of Science

ACKNOWLEDGEMENTS

The work presented in this thesis was performed at the Department of Biological Sciences at the University of Bergen between January 2022 and November 2022.

Firstly, I would like to thank my amazing supervisor Aurélia E. Lewis for her support and kindness and assistance throughout the period of this project. I am grateful for your willingness to answer all the questions I have whenever I come disturb you in your office and for your patience when I was writing. You are deeply appreciated. I would also like to thank my co-supervisor Sushma Grellscheid for agreeing to be part of my master's project even though we only got to speak once and introduce ourselves.

Secondly, I would like to thank Diana C. Turuc. You have been a great teacher in the lab. Thank you for always ready to teach and help me with the lab work and for always ready to troubleshoot experiments with me when things did not go as planned. I am grateful for your help.

I would also like the thank Sandra Ninzima for helping in the cell lab and with the little things around the lab. In addition, I would like to thank Andrea Morovicz for helping with the quantification programs. Thank you so much for all the help you have all given me. I do not take them for granted. I would also like to thank everyone on the 5th floor who has helped me in any way during my project.

I would like to thank my office mate Farha Omer. Talking about everything with you made the whole master experience less lonely. Thank you for always willing to help me.

Lastly, I would like to thank my family and friends for supporting me through this master journey, I really appreciate everyone.

TABLE OF CONTENTS

SELECTED ABBREVIATIONS

PTB	Polypyrimidine tract-binding protein
mRNA	Messenger ribonucleic acid
RRM	RNA recognition motif
NLS	Nuclear localisation signal
NES	Nuclear export sequence
PML	Pro-myelocytic leukaemia
PNC	Perinucleolar compartment
GFP	Green fluorescent protein
RNA pol II	RNA polymerase II
PPIns	Polyphosphoinositides
PtdIns	Phosphatidylinositol
PI4-kinase	Phosphatidylinositol 4-kinase
PI4KIIIβ	Phosphatidylinositol 4-kinase type IIIβ
PIP5KIα	Phosphatidylinositol 4-phosphate 5-kinase type Iα
PI 5 phosphatase	Phosphoinositide 5 phosphatase
PI3K p110β	Class IA phosphoinositide 3-kinase catalytic subunit p110β
PtdIns(4,5)P_2	Phosphatidylinositol 4,5-biphosphate
PtdIns(3,4,5)P_3	Phosphatidylinositol 3,4,5-triphosphate
DNA	Deoxyribonucleic acid
SDM	Site directed mutagenesis
GST	Glutathione S-transferase
INPP5K(SKIP)	Inositol polyphosphate-5-phosphatase K
WT	Wild type

ABSTRACT

Polypyrimidine tract binding protein 1 (PTB) is an extensively expressed RNA binding protein that regulates alternate splicing of exons in the nucleus. PTB is also localized in a nuclear body called perinucleolar compartment (PNC) that is predominantly present in aggressive cancer cells. PTB has been reported to be overexpressed in cancer cells and significant knockdown of PTB has been shown to inhibit cell proliferation while PNC has also been linked to regulating cancer cell gene expression, thereby suggesting the PNC as a biomarker for cancer**.**

Polyphosphoinositides (PPIns) are membrane signalling lipids that interact with different proteins via electrostatic interactions. Some of these PPIns have been found to localize in the nucleus where they contribute to cellular processes including transcription and mRNA splicing, alongside their effector proteins. Previous reports from our group have shown that two different PPIns (PtdIns(4,5)P_2 and PtdIns(3,4,5)P_3) interact with PTB in the nucleus via an interatomic study. In addition, our group confirmed the direct binding of several PPIns to PTB *in vitro* and further identified two residues involved in the binding, K439 and K440.

Here, we generated an additional residue R437L mutation in the full length PTB-K439A-K440L via site directed mutagenesis to assess its PPIn binding properties to PTB, but we were not able to express the protein. Additionally, we assessed the localization of the PTB-R437L-K439A-K440L mutant *in vitro* in comparison to WT PTB in the endometrial cell line MFE-319. Furthermore, we focused on regulating PTB protein expression levels. We showed that nuclear PI3K p110β activity (a PtdIns(3,4,5)P_3-generating enzyme) may be involved in regulating PTB protein levels. Alternatively, we overexpressed a PI 5-phosphatase SKIP, in the nucleus to investigate the role PtdIns(4,5)P_2 plays in regulating PTB levels but the fusion of the protein NLS-EGFP-SKIP did not express and so we were unable to examine PTB protein levels.

This study hypothesized based on existing evidence that PtdIns(4,5)P_2 may be involved in regulating PTB protein levels however, our result suggests that PI3K p110β activity may contribute to regulating PTB protein expression levels in the nucleus.

1.0 INTRODUCTION

1.1 Polypyrimidine tract-binding protein 1

Polypyrimidine-tract-binding protein 1 (PTB), also known as heterogeneous nuclear ribonucleoprotein I (hnRNPI), is a 52 k Da RNA-binding protein that contains 531 amino acids (Sawicka et al. 2008). This protein binds directly to pyrimidine-rich RNA sequences that have repeated sequences of cytosine and uracil, preferably UCU and CUC triplets (Babic, Sharma, and Black 2009). PTB is mainly localized in the nucleus, however, it can shuttle between the nucleus and the cytoplasm (Perez, McAfee, and Patton 1997; Kamath, Leary, and Huang 2001; Li and Yen 2002). Depending on where it is localized, PTB regulates various cellular functions. For example, in the cytoplasm, it regulates messenger ribonucleic acid (mRNA) metabolism which includes mRNA stability, translation, and localization (Sawicka et al. 2008). While in the nucleus, it is involved in the regulation of alternative splicing (AS) of exons (Garcia-Blanco, Jamison, and Sharp 1989). The importance of this process, splicing, has been emphasized over the years (Darnell 2013). In a simple term, splicing means removing the non-protein coding DNA sequences called introns, and the remaining sequences called exons are connected during the process. During pre-mRNA splicing, the act of removing or adding specific exons to derive various types of protein from the same pre-mRNA is called alternate splicing (Wang et al. 2008). It has been confirmed that greater than 90% of human genes undergo alternative splicing (Pan et al. 2008).

PTB consists of four RNA-binding domains that allow easy interaction with RNA sequences. These domains are better known as RNA recognition motifs (RRMs) [figure 1], and they are separated by interdomain linker regions and an N-terminal extension where nuclear localization signal (NLS) and nuclear export signal (NES) are present (Romanelli et al. 1997). RRM1 and 2 are involved in PTB dimerization, while RRM3 and 4 are involved in high affinity interaction with RNA(Wang et al. 2008). These RRMs not only help to identify protein-protein and/or protein-lipid interactions between the splicing factors but also add to the interpretation of RNA recognition potential (Romanelli, Diani, and Lievens 2013). Although each of these RRMs binds to pyrimidine-rich sequences, the binding occurs at a different RNA-binding site (Sawicka et al. 2008). How PTB regulates its functions in the nucleus is yet to be understood however different models has been reported (Romanelli, Diani, and Lievens 2013). In addition to its various molecular functions, PTB has appeared to play an important role in pre-mRNA splicing in cancer (Cheung et al. 2009).

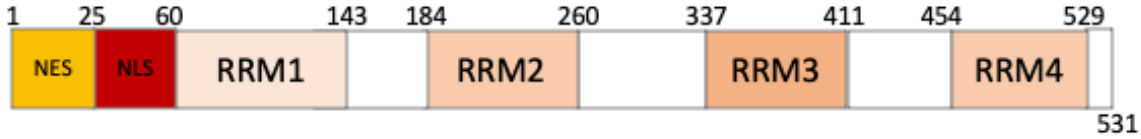

Figure 1: The schematic representation of Polypyrimidine-tract-binding protein 1. PTB consists of four RNA recognition motifs with their amino acids' positions: RRM1 (60-143), RRM2 (184-260), RRM3 (337-411) and RRM4 (454-529) respectively. The overlapping nuclear export sequence (NES 1-25) and nuclear localization signal (NLS 1-60) are located at the N-terminal extension of the protein. This figure was made using BioRender.

1.1.1 PTB in Cancer

1.1.1.1 Alternative splicing in cancer

AS is an important mechanism eukaryotic cells use to increase their proteome diversity from limited types and/or classes of genes. But in pathological cases where these genes are abnormally spliced, particularly in cancer, can lead to an aberrant functioning of a cell. Cancer-specific splicing occurrences have been reported at the mRNA level in different tissues (Wang et al. 2017). Abnormal splicing events in cancer has been reported as one of the leading causes of tumour initiation and oncogenes. AS has greatly affected protein levels and function (Takahashi et al. 2015).

1.1.1.2 PTB expression and function in cancer

PTB has been reported to be overexpressed in cancer cells and these expressions may be partially involved with aberrant splicing (He et al. 2007) although, the overall effect of PTB on cancer cell malignancy depends on the cell type (Romanelli, Diani, and Lievens 2013). In human epithelial ovarian cancer (He et al. 2007), breast cancer (Takahashi et al. 2015), different malignant cell lines (Wang et al. 2008), and in a wide array of glia-derived tissue (McCutcheon et al. 2004), reports have shown that PTB is overexpressed. These expressions, therefore, have been associated with the growth and maintenance of transformed properties in ovarian cancer (He et al. 2007). Consistently, significant knockdown of PTB expression in cancer cells by small interfering-RNA with reference to ovarian (Wang et al. 2018) and breast cancer (Takahashi et al. 2015) have inhibited proliferation, anchorage-dependent growth and cell invasion (Romanelli, Diani, and Lievens 2013).

Cancer cells exhibit at least four enhanced cellular processes, namely, proliferation, survival, motility, and invasion (Hanahan and Weinberg 2000), these processes are also relatively involved in genes PTB alternatively splice. These genes include fibroblast growth factor receptor 1 & 2, *FGFR1 & 2* involved in proliferation, Fas cell surface Death receptor *FAS,* and Caspase 2 *CASP2*, involved in apoptosis, Proto-oncogene tyrosine-protein kinase Src *CSRC*, involved in invasion and Alpha-actinin-3 *ACTN3,* & fibrillin-1 *FBN1*, involved in motility (Romanelli, Diani, and Lievens 2013).

1.1.2 PTB and Perinucleolar compartment

The nucleus is a highly organized and complex organelle that controls gene expression, DNA replication and repair, RNA processing and splicing, and various other functions. These functions however are highly compartmentalized into nonmembrane-bound nuclear domains and nuclear bodies which include nucleoli, pro-myelocytic leukaemia (PML) bodies, nuclear speckles, and perinucleolar compartment (PNC), to mention a few. The PNC is located at the nucleolar periphery and it has been reported that the PNC was originally described by the localization of PTB in these foci [figure 2] (Pollock and Huang 2009). PNC is predominantly present in cancer cells and its prevalence in normal cell lines is low (Huang et al. 1997). The PNC is composed of several non-coding RNAs and proteins. These proteins are important in pol II RNA metabolism (Pollock and Huang 2010).

According to Huang *et al.* (Huang et al. 1997), RNA binding is said to be essential in the localization of PTB in the PNC as the study showed that out of the four RRMs of PTB, at least three are required for GFP-PTB fusion protein to be targeted to the PNC using a deletion mutagenesis method. Although the function of the PNC is yet to be completely understood, however, studies have shown that PNC forms in a wide range of cancer cells thereby regulating their gene expression, this thereby suggested PNC as a biomarker for cancer (Pollock and Huang 2010, 2009).

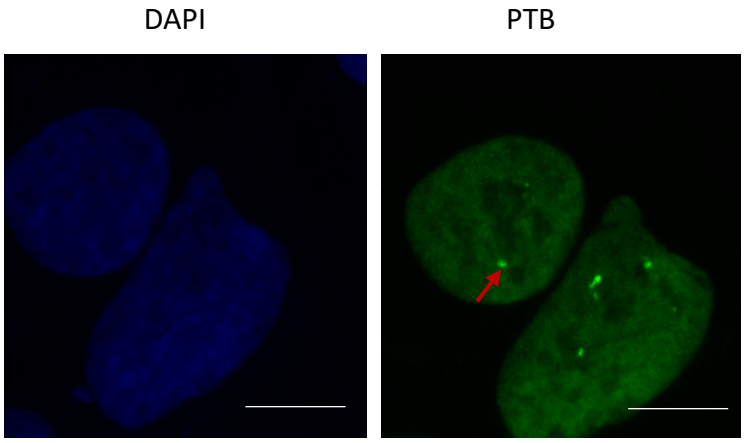

Figure 2: Localization of PTB in Perinucleolar compartment. MFE-319 cells were stained with anti-PTB antibody and imaged using fluorescent microscopy at 100X magnification. The cells were stained with DAPI to detect the nuclei. PTB foci is represented with the green dot (arrowhead) indicating the presence of the PNC. The scale bar is 5 μm.

1.2 Polyphosphoinositides

Polyphosphoinositides (PPIns) are a small class of membrane phospholipids that are found in eukaryotic cells. Although PPIns occupy a small portion of all the phospholipids at large, they play an essential role in signal transduction pathways in the cell (Toker 2002). PPIns are reversibly phosphorylated derivatives of phosphatidylinositol (PtdIns). PPIns are amphiphilic, which means that they have two non-polar fatty acyl chains esterified to their glycerol backbone and a polar inositol head group that is attached via a phosphodiester bond. This inositol headgroup has three free hydroxyl groups on positions 3, 4 and 5 of the inositol rings that can be phosphorylated by specific lipid kinases [figure 3]. The resulting phosphorylation yield seven different PPIns with different structures and anionic charge. They include three mono-phosphorylated PtdIns3*P*, PtdIns4*P*, and PtdIns5*P*, three di-phosphorylated PtdIns(3,4)P_2, PtdIns(4,5)P_2 and PtdIns(3,5)P_2 and lastly, a tri-phosphorylated PtdIns(3,4,5)P_3 (Dickson and Hille 2019).

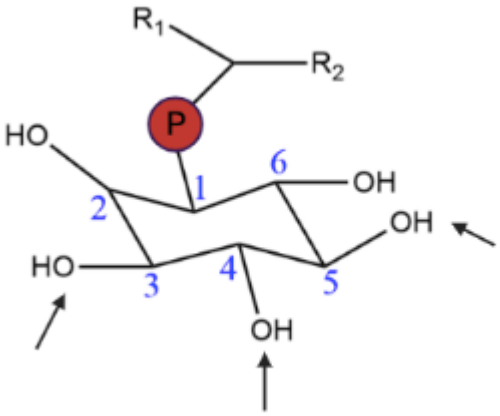

Figure 3: Chemical structure of the phosphatidylinositol headgroup. Phosphatidylinositol is a glycerophospholipid that contains two non-polar fatty acyl chains represented with R-groups (R_1 usually a saturated fatty acid and R_2, a non-saturated fatty acid) esterified to the glycerol backbone, and a polar inositol ring attached via a phosphodiester bond (represented with the red circle P). The arrow heads indicate the three hydroxyl-groups on the inositol headgroup where phosphorylation takes place resulting in the seven different polyphosphoinositides. This figure was made using ChemDraw.

1.2.1 Polyphosphoinositides-protein Interaction

PPIns are anionic lipids that play a significant role in the recruitment of cationic proteins to the membrane interface through electrostatic interactions (Stahelin, Scott, and Frick 2014). These proteins are often referred to as peripheral proteins. The spatial distribution and the appearance of each of the mono-, bis-, and tri-phosphorylated derivatives of PtdIns serve as an important aspect of how they communicate their information to target proteins (Stahelin, Scott, and Frick 2014). These proteins bind to PPIns through specific domains they possess. Pleckstrin homology (PH) domain was one of the first PPIn-binding domain to be discovered. PH domain can interact with PtdIns (3,4)P_2, PtdIns (4,5)P_2, and PtdIns (3,4,5)P_3 (Lemmon 2008). Along a variety of other PPIn-binding domains discovered after PH domain is the FYVE domain. FYVE domain mostly interacts with PtdIns3P (Kutateladze 2010). Proteins representing these domains coordinates various PPIns headgroups they interact with and then translocate them to their specific membrane interaction sites in the cell (Lemmon 2008). In addition to protein domains, PPIns also targets proteins with polybasic regions (PBR) or KR-motifs to the plasma membrane, which contain four or more basic residues. KR-motifs contain a sequence pattern: K/R-($X_{n=3-7}$)-KXKK, which were shown to interact with PtdIns(4,5)P_2 and PtdIns (3,4,5)P_3 (Heo et al. 2006; Karlsson et al. 2016).

1.2.2 Polyphosphoinositides in the Nucleus.

PPIns exist both in the nuclear envelop and in the interior of the nucleus, even though their physicochemical structure and presentation is yet to be fully understood (Shah et al. 2013). PPIns were first discovered in the plasma membrane, however, after a decade, they were discovered within the nucleus (Jacobsen et al. 2019). Ever since this discovery, further studies have shown evidence to the localization of PPIns in the nucleus as well as identifying effector proteins these PPIns interact with to further understand their role in the nucleus (Jacobsen et al. 2019). Apart from PtdIns(3,5)P_2, all other PPIns have been discovered in the nucleus. Some of these PPIns (PtdIns4P, PtdIns(3,4)P_2, and PtdIns(4,5)P_2) have been identified in a non-membrane bound nuclear domain called nuclear speckles [figure **4**]. These speckles are where pre-mRNA splicing components are located, and they can be found in the nucleoplasm along the interchromatin (Spector and Lamond 2011).

PtdIns(4,5)P_2 is the most abundant PPIns (Dickson and Hille 2019) and is one of the first PPIns to be discovered, in the nucleus. It has been found to be predominantly localized in the nuclear speckles [figure 4**B**] where it co-localizes with some enzymes that are important components for both the transcriptional events and pre-mRNA processing machinery. An example of such enzyme is RNA polymerase II (Osborne et al. 2001). PtdIns(3,4,5)P_3, on the other hand, have been found to be localized in both the nucleoplasm and nucleolus (Jacobsen et al. 2019). PtdIns(3,4,5)P_3, alongside its interaction with effector and nuclear proteins mediates anti-apoptotic effects of nerve growth factor (NGF) and contributes to cell survival upon the activation of PI3K and Akt (Shah et al. 2013; Jacobsen et al. 2019).

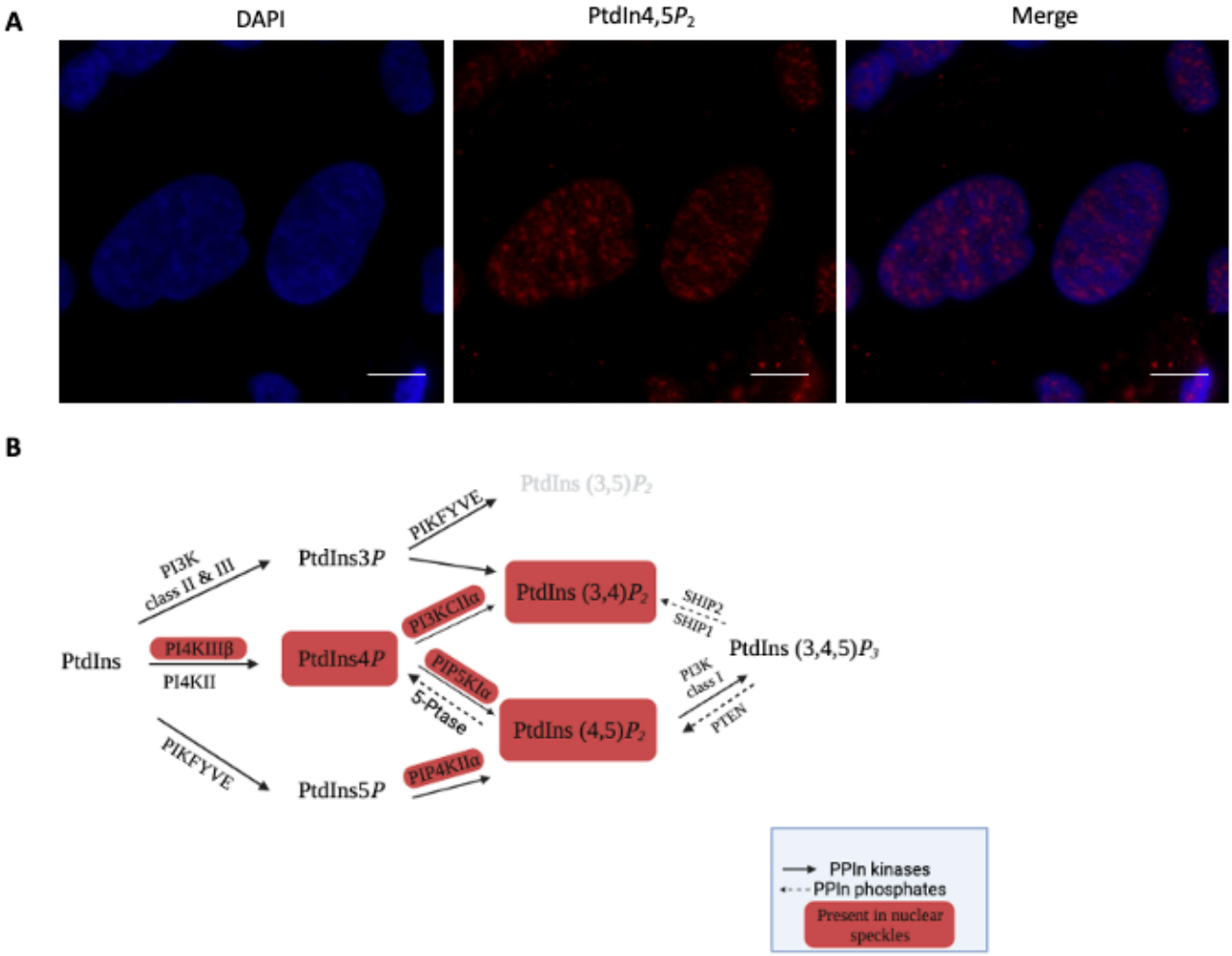

Figure 4: Polyphosphoinotides (PPIns) metabolism in nuclear speckles. (**A**) Localization of PtdIn4,5P_2 in the nuclear speckles. MFE-319 cells were stained with anti- PtdIn4,5P_2 antibody and imaged using fluorescent microscopy at 100X magnification. The cells were stained with DAPI to detect the nuclei. PtdIns(4,5)P_2 (red) showing distinct foci in the nuclear speckles. The scale bar is 5 µm. (**B**) PPIns metabolism in nuclear speckles. All the seven different PPIns and how they are regulated via specific kinases and phosphatases in the nucleus excluding PtdIns(3,5)P_2 are shown. The PPIns and enzymes highlighted in red have been found to be localised in the nuclear speckles (Shah et al. 2013).

1.2.3 PtdIns(4,5)P_2 and PtdIns(3,4,5)P_3 metabolism in the nucleus.

PtdIns(4,5)P_2 is metabolized in the nuclear speckles due to the presence of a series of kinases and likewise regulated by phosphatases. PtdIns(4,5)P_2 can be synthesized from PtdIns via two steps. First, a type III PtdIns4-kinase isoform β (PI4KIIIβ) produces PtdIns4P and secondly, a PtdIns4P 5-kinase (PIP5KIα) acts on PtdIns4P to produce PtdIns(4,5)P_2 (Falkenburger et al. 2010) [Figure 4**B**]. In addition, PtdIns(4,5)P_2 can also be synthesized from type II PIP4Kα acting upon PtdIns5P [figure 4**B**]. Alternatively, PtdIns(4,5)P_2 can be obtained via a dephosphorylation by a PI 5-phosphatase [5-Ptase in figure 4**B**] (Jacobsen et al. 2019).

PtdIns(4,5)P_2 regulates quite a number of cellular processes in the nucleus through its interaction with effector proteins, including transcriptional regulation, splicing (Shah et al. 2013).

PtdIns(3,4,5)P_3 is synthesized following an activation of class IA phosphoinositide 3-kinase catalytic subunit p110β (PI3K-p110β) which phosphorylates PtdIns(4,5)P_2 on the position 3 of the inositol ring in the nucleus and nucleolus [figure 4**B**] (Jacobsen et al. 2019; Falkenburger et al. 2010).

1.2.4 Influence of PtdIns(4,5)P_2 and PtdIns(3,4,5)P_3-protein interaction on nuclear localisation.

Studies have reported that PtdIns(4,5)P_2 and PtdIns(3,4,5)P_3 may be linked to influencing the nuclear localisation of some of their effector proteins by inducing conformation changes that causes their redistribution within the nucleus (Jacobsen et al. 2019). This is possible because of the PBR or K/R motifs these proteins possess that is similar to NLS sequence (Jacobsen et al. 2019). For instance, PtdIns(4,5)P_2 and its metabolizing enzyme, PIP5KIα upon interacting with the polybasic motif in the C-terminal regulatory domain of tumour suppressing protein p53, regulates its stabilization in the nucleus (Choi et al. 2019). Subsequently, PtdIns(4,5)P_2 and PtdIns(3,4,5)P_3 binding can translocate nuclear effector proteins from the nucleus to the cytoplasm when disrupted (Jacobsen et al. 2019). For example, mutation of the PBR that binds PtdIns(4,5)P_2 to p53 causes a high distribution levels of p53 in the cytoplasm (Choi et al. 2019) likewise, a PtdIns(3,4,5)P_3-binding protein, upon the introduction of constitutively active PI 3-kinase in the nucleus, is also translocated to the cytoplasm. This protein is necessary for PtdIns(3,4,5)P_3 binding in the nucleus (Jacobsen et al. 2019).

1.2.5 PtdIns(4,5)P_2 and PtdIns(3,4,5)P_3 functions within the nucleus.

The functions of nuclear PPIns have been attributed to their interacting partners as they provide the importance of how these nuclear PPIns influence diverse key nuclear processes (Jacobsen et al. 2019). Few of the functions these PPIns alongside their interactions with effector proteins is summarized below.

Nuclear PtdIns(4,5)P_2 in mRNA processing and export

PtdIns(4,5)P_2 has been implicated either in the direct or indirect interaction with effector proteins that play crucial roles in the nucleus (Jacobsen et al. 2019). Localization of PtdIns(4,5)P_2 in nuclear speckles has been reported to be involved in the regulation splicing events *in vitro* (Shah et al. 2013). PtdIns(4,5)P_2 interacts with components of small nuclear ribonucleoproteins (RNP) as well as the splicing factor SC-35, involved in mRNA processing. It was reported that immunodepletion of PtdIns(4,5)P_2 inhibited pre-mRNAs splicing *in vitro* (Osborne et al. 2001; Jacobsen et al. 2019).

Nuclear PtdIns(*3,4,5)P_3 in cell survival*

Nuclear PtdIns(3,4,5)P_3 and PI3K activity has been reported to mediate the anti-apoptotic effects of the nerve growth factor (NGF) alongside its interaction with nucleophosmin (also known as B23). The nuclear PtdIns(3,4,5)P_3 regulates nucleophosmin-caspase-activated DNase (CAD) interactions and subsequently inhibits DNA fragmentation activity of CAD (Jacobsen et al. 2019; Ahn et al. 2005). Another nuclear protein that contributes greatly to cell survival is GTPase phosphatidylinositol 3-kinase (PIKE)-L via its interaction with PtdIns(3,4,5)P_3 (Jacobsen et al. 2019).

1.3 Background work with PTB

PTB is one of the several proteins involved in splicing our group found that interacts with and binds to PPIns in the nucleus. Through mass spectrometry-based interactomics, PTB was identified as a PtdIns(4,5)P_2 and PtdIns(3,4,5)P_3 interacting protein (Lewis et al. 2011; Mazloumi Gavgani et al. 2021). Further investigations by our group showed that the part containing the RRM3, and the linker C-terminal of the motif was the only fragment (F3) that interacted with PPIns compared to all the regions of the protein [unpublished data, shown in figure 5**D**]. Our group extended the investigations to further determine the exact residues responsible for the interaction by performing site-directed mutagenesis on the RRM3-linker fragment. Two possible locations were found each containing two lysines (K373-K374 & K439-K440) and were mutated to uncharged residues. The mutants were expressed and subjected to a lipid overlay assay, it was then observed that only K439A-K440L mutants reduced all the PPIn-binding lipids to F3 [figure 5**E**]. However, when these mutants were examined in the full length of the protein, only a partial reduction of the binding was observed [figure 5**F**] thus, indicating that some other residues share these PPIns binding attributes to

PTB. Potential residues that might be involved in the remaining PPIn binding include arginine at position 437 and the lysine at position 444 because they are in close proximity with the mutated lysines sequence-wise and are solvent accessible [figure 5**C**].

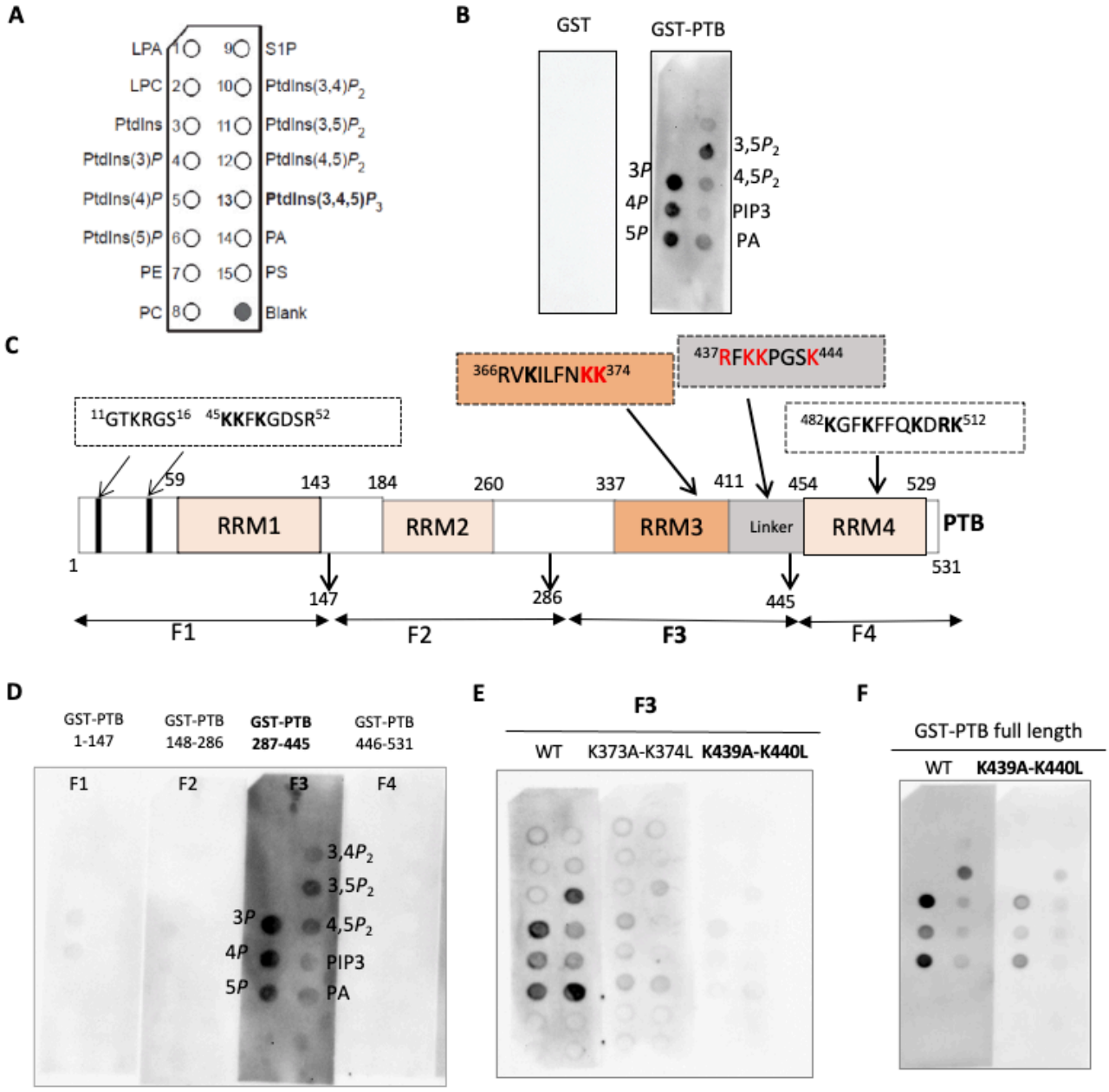

Figure 5: Schematic overview of Lipid overlay assay showing PPIns interactions with GST-PTB WT and K373A-K374L, K439A-K440L mutants. (A), PIP strip schematic (www.echeloninc.com) showing the positions of the following glycerophospholipids: lysophosphatidic acid (LPA), lysophosphocholine (LPC), phosphatidylinositol (PtdIns), PtdIns3*P*, PtdIns4*P*, PtdIns5*P*, phosphatidylethanolamine (PE), phosphatidylcholine (PC), sphingosine-1-phosphate (S1P), PtdIns(3,4)P_2, PtdIns(3,5)P_2, PtdIns(4,5)P_2, PtdIns(3,4,5)P_3, phosphatidic acid (PA), phosphatidylserine (PS) and blank. (**B**), PPIns strips showing the binding of GST and GST-PTB WT FL- to different phospholipids. (**C**), a schematic representation of PTB highlighting the four RRMs, the C-terminal linker of the motif, positions of their amino acids and the fragments to which the RRMs were divided (**4**). The residues coded in red are the residues (K373-K374, K439-K440) that were mutated to uncharged residues and potential residues that might be involved in the binding (R437& K444). (D), PPIns strips showing the binding of GST-RRM1 (**F1**), RRM2 (**F2**), RRM3 (**F3**), and RRM4 (**F4**) to different phospholipids. GST- RRM3 (**F3**) is the only fragment that showed PPIn interaction. **(E)**, PPIns strips showing the binding of GST-RRM3 fragment, K373A-K374L, and K439A-K440L mutants to different phospholipids. (**F**), PPIns strips showing the binding of GST-PTB FL-WT and K439A-K440L mutants to different phospholipids. Unpublished data carried out by previous members of the AE Lewis group.

1.4 Aim of the Study.

The goal of this study was divided into two parts. The first part further aimed to generate a full PPIn binding mutant and examine its subcellular localization while the second part was directed to study the regulation of the PTB protein levels by PPIns.

In the first part of this study, we aimed to build upon the effect of double-mutated PTB (PTB -K439A-K440L) on PPIn interaction. By doing so, we aimed to generate a full PPIn binding mutant by mutating R437 by site-directed mutagenesis (SDM) and to test its effect on PPIn binding by lipid overlay assay. Additionally, we aimed to generate EGFP-tagged PTB -R437L-K439A-K440L construct by SDM to examine its subcellular localization compared to WT using transient transfection and microscopy.

In the second part, we studied the regulation using two approaches. First, we manipulated the levels of PPIn by inhibiting the metabolic kinases localised in the nucleus via the pathway focused around PtdIns(4,5)P_2 and PtdIns(3,4,5)P_3 following a measure of nuclear PTB levels.

Secondly, we overexpressed a PI 5-phosphatase SKIP in the nucleus with the aim of decreasing nuclear PtdIns(4,5)P_2 levels.

Aims:

- To generate an additional mutation R437L in the full length PTB-K439A-K440L and to investigate its effect on PPIn interaction and subcellular localization compared to WT PTB in cancer cells.
- To investigate the effect of PIP5Kα and PI3K p110β inhibition in regulating PTB protein levels in cancer cells.
- To manipulate the levels of PtdIns(4,5)P_2 in the nucleus to investigate the role of PtdIns(4,5)P_2 in regulating PTB protein levels.

2.0 MATERIALS AND METHODS

2.1 MATERIALS

The materials are arranged alphabetically.

Table 2.1.1 Agarose Gel Electrophoresis

1x TAE Buffer	6x DNA Sample Buffer
40 mM Tris base	30% Glycerol
1 mM EDTA pH 8.0	0.025% Bromophenol blue
20 mM Acetic acid	

Table 2.1.2 Antibodies

Name	Supplier	Dilution	Type	Catalog#	Lot#
α-PTB	Abcam	1:200 IF	Rabbit-monoclonal IgG	Ab133734	GR97937
α-Ptdlns(4,5)P_2	Invitrogen	1:200 IF	Mouse-monoclonal IgM	MA3-500 (2C11)	UC282853
Goat α-mouse Alexa Fluor® 594-conjugated	Invitrogen	1:200 IF	IgM (μ-chain)	A21044	1934085
Goat α-mouse Alexa Fluor® 594-conjugated	Invitrogen	1:200 IF	IgG (H+L)	A11005	1937185
Goat α-rabbit Alexa Fluor® 488-conjugated	Invitrogen	1:500 IF	IgG (H+L)	A11008	1885240
Goat α-rabbit-horseradish peroxidase	Life Technologies	1:10000 WB	IgG (H+L)	G21234	1744754
Goat α-mouse-horseradish peroxidase	Invitrogen	1:10000 WB	IgG (H+L)	G21040	2185072

*α-anti, IF-immunofluorescence, WB-Western immunoblotting

Table 2.1.3 Bacteria

Chemical	Supplier	Purpose
Escherichia coli XL1-Blue Supercompetent Cells	Invitrogen	Cloning
Escherichia coli BL-21 CodonPlus® (DE3)-RIL competent cells	Agilent	Protein expression

Table 2.1.4 Bacteria Culture

LB medium	LB agar
1% (w/v) tryptone 0.5% (w/v) yeast extract 1% (w/v) NaCl	1.5% (w/v) agar in LB medium

Table 2.1.5 Cell Culture Reagents

Chemical	Supplier
Dulbecco's modified eagles's medium (DMEM) (containing L-Glu & 4.5g Glucose)	Sigma
Foetal bovine serum (FBS)	Sigma
100x Penicillin-Streptomycin (PEN/STREP)	Echelon

Table 2.1.6 Cell Lines

Chemical	Supplier
Ishikawa	HB Salvesen, K2, UiB
HeLa	M.Bakke, ATCC
MEF-319	HB Salvesen, K2, UiB

Table 2.1.7 Chemicals

Chemical	Abbrev. /Formula	Supplier	Grade Purity	Catalog #
2-amino-2-hydroxymethyl-1,3-propanediol, Trizma® base	Tris	Sigma	ANG	T6066
30% Acrylamide/Bis-acrylamide		Bio-Rad		161-0158
4-(1,1,3,3-Tetramethylbutyl) phenyl-polyethylene glycol	Triton® X-100	Sigma	MBG	T8787
Acetic acid	CH_3COOH	Sigma		33209
Agarose, SeaKem® LE		Lonza	ELG	50004
Ammonium persulfate	APS	Bio-Rad		161-0700
Ampicillin, ready-made solution	Amp	Sigma		050M4075
Bacto™ Tryptone		BD	MBG	BD 211705
Bacto™ Yeast Extract		BD	MBG	BD 212750
Bovine serum albumin	BSA	Sigma		A7906
Bovine serum albumin, essentially fatty acid free	BSA	Sigma	≥96%	A6003
Bromophenol blue	BPB	Merck		L59076322
Calcium chloride	$CaCl_2$	Merck		1.02083
Dimethylsulfoxide	DMSO	Sigma		D2650
DL-Dithiothreitol	DTT	Sigma		D9163
Ethanol	EtOH	Kemetyl		600051
Glycerol		Merck	85%	1.04094
Glycerol, Ultra-pure		Invitrogen	≥99.5%	15514-011
Isopropanol	IPA	Kemetyl		600079

Isopropyl-B-D-thiogalactopyranos-ide	IPTG	Apollo Scientific		BIMB1008
LB-agar		Sigma	MGB	L7025-TAB
L-glutathione, reduced		Sigma-Aldrich	≥98%	G4251
Magnesium chloride	$MgCl_2$	Merck	ANG	1.05833
Methanol	MeOH	Sigma		32212N
N, **N, N**',N'-tetramethylethane-1,2-diamine	Temed	Bio-Rad		161-0800
Paraformaldehyde	PFA	Merck		K40988605
Polyoxyethylenes orbitan monolaurate	Tween®20	Sigma-Aldrich		P1379
Potassium chloride	KCl	Merck	ANG	1.04936
Prolong™ Glass antifade mountant with NucBlue™	DAPI	Invitrogen		P36985
Sodium chloride	NaCl	Sigma-Aldrich	≥99.8%	31434N

*ANG- analysis grade, DAPI – 4',6-diamidino-2-phenylindole, ELG – electrophoresis grade, MBG – molecular biology grade.

Table 2.1.8 Commercial Buffers & Reagents

Chemical	Purpose	Supplier
0.5 M Tris-HCl pH 6.8	SDS-PAGE	Bio-Rad
0.5 M Tris-HCl pH 8.8	SDS-PAGE	Bio-Rad
Calf intestinal alkaline phosphate 10x buffer	Cloning	NEB
Sequencing buffer	Sequencing	UiB Sequencing Lab
SDS solution 20% (w/v)	SDS-PADE	Bio-Rad

Table 2.1.9 Commercial Kits

Name	Purpose	Supplier
BCA Reagent	Protein quantification	Pierce
NucleoSpin® Gel and PCR Clean-up	DNA extraction and purification	Macherey-Nagel
NucleoSpin® Plasmid	Plasmid purification	Macherey-Nagel
NucleoSpin® Xtra Midi	Large scale Plasmid purification	Macherey-Nagel
Phusion® High-Fidelity DNA polymerase	Cloning	Finn-zymes
Protein Assay Dye Reagent Concentrate	Protein quantification	Bio-Rad

Table 2.1.10 Equipment

Name	Software	Purpose	Supplier
AllegraX-12R centrifuge			Beckmann Coulter
Alpha™ Unit Block Assembly for DNA Engine® System		PCR	Bio-Tek
Avanti™J-25 Centrifuge			Beckmann Coulter
ChemiDoc XRS+™	ImageLab	Blots & SDS-PAGE IMG	Bio-Rad
Epoch-Microplate Spectrophotometer w/Take3 plate	Gen5	DNA & Protein concentration	Bio-Tek
Eppendorf-Centrifuge 5810			Eppendorf
Flow bench VD 2040S			OAS Laf
Fluorescence microscope DMI 6000B	Leica Application Suite IFv2		Leica

Galaxy-MiniStar Centrifuge			VWR
GelDoc EZ Imager	ImageLab	Native gel IMG	Bio-Rad
Liquid Nitrogen storage system			Thermolyne
Microcentrifuge			VWR Hitachi Koki Co., Ltd
Ultrasonic Homogenizer 4710 Series			Cole-Palmer Instrument Co.
UV illuminator TFP35M			Vilbur Lourmat
Water bath GD100			Grant

*PCR – Polymerase chain reaction, IMG – Imaging

Table 2.1.11 Plasmids

Name	Supplier	Restriction Sites (5'-3')
EGFP-C1	Addgene	-
EGFP-C1-PTB	Previous study from A. Midlang	Xho1, EcoR1
EGFP-C1-PTB-K439A-K440L	Previous study from A. Midlang	Xho1, EcoR1
EGFP-C1-PTB- R437L-K439A-K440L	This study (IA. Oyediran)	Xho1, EcoR1
pGEX4T1-PTB*	Christopher WJ Smith (University of Cambridge, UK)	Unknown*
pGEX4T1-PTB-R437LK439AK440L*	This study (IA. Oyediran)	Unknown*

pBABE-EGFP-NLS-SKIP WT or PD (D269A)	D Mann Imperial college London	Nhe1, EcoR1, Bgl11
pProTαNLS-EGFP	This study (IA. Oyediran)	-
pProTαNLS-EGFP (ATG->TTG)	This study (IA. Oyediran)	-
pProTαNLS-EGFP-SKIP WT or PD (D269A)	This study (IA. Oyediran)	-
pProTαNLS-EGFP (ATG-> TTG) -SKIP WT or PD	This study (IA. Oyediran)	-

* We verified the PTB sequence using sequencing, however, the exact pGEX vector PTB was cloned into is unknown but has been used from the lab we got it from in publications.

Table 2.1.12 Primers

Name	Sequence 5' to 3'	Application
EGFPC1-NLS-SKIP-BglII Forward	TCCGGACTCAGATCTATGAGCTCGCGGAAGCTG	In fusion cloning
EGFPC1-NLS-SKIP-EcoRI Reverse	GTCGACTGCAGAATTCTCAGATCTGTGGCTGTGCTTC	In fusion cloning
EGFPC1-NLS-SKIP-ATG Forward	CCACCTTGGTGAGCAAG	SDM
EGFPC1-NLS-SKIP-ATG Reverse	CTTGCTCACCAAGGTGG	SDM
PTB-R437L Forward	CTCACCCCTGCACCTCTTCGCGCTGCCGG	SDM
PTB-R437L Reverse	CCGGCAGCGCGAAGAGGTGCAGGGGTGAG	SDM
EGFPC2 forward	CGAGAAGCGCGATCACATGG	Sequencing/ Colony PCR
EGFPC2 Reverse	GGACAAACCACAACTAGAATGCAG	Sequencing/ Colony PCR
pGEX forward	GGGCTGGCAAGCCACGTTTGGTG	Sequencing
pGEX reverse	CCTCTGACACATGCAGCTCCCGG	Sequencing

Red – restriction sites, Blue – Extra nucleotide in frame, Green – SKIP sequence, Yellow – mutated nucleotide.

Table 2.1.13 Protein Purification

Lysis Buffer	Elution Buffer
1x PBS pH 7.4	50 mM Tris pH 7.6
500 mM NaCl	500 mM NaCl
2 mM DTT	10 mM KCl
10% glycerol	10 mM $MgCl_2$
10 mM KCl	2 mM DTT
10 mM $MgCl_2$	4% glycerol
1:100 Protease inhibitor cocktail	20 mM reduced L-glutathione
0.5% NP 40	
Wash Buffer	**1x PBS pH 7.4**
1x PBS pH 7.4	137 mM NaCl
10 mM KCl	2.68 mM KCl
2 mM DTT	8 mM $Na_2HPO_42H_2O$
10% glycerol	
10 mM $MgCl_2$	
500 mM NaCl	

Table 2.1.14 SDS-PAGE & Western Blotting

Resolving gel	Stacking gel
10-12% of 30% acrylamide/bis-acrylamide (37.5:1)	5% of 30% acrylamide/bis-acrylamide (37.5:1)
375 mM Tris-HCl pH8.8	125 mM Tris-HCl pH 6.8
0.1% (v/v) SDS	0.1% (v/v) SDS
0.1% (v/v) APS	0.1% (v/v) APS
0.04% (v/v) *TEMED*	0.1% (v/v) *TEMED*

5x SDS Sample Buffer	**1x PBS-T pH 7.4**
65 mM Tris-HCl pH 6.8	137 mM NaCl
5% SDS (v/v)	2.68 mM KCl
250 mM DTT	8 mM $Na_2HPO_42H_2O$
20% glycerol	0.05% (v/v) Tween 20
0.2% Bromophenol blue (w/v)	

1x Running Buffer	**1x Transfer Buffer**
25 mM Tris HCl pH 8.3	25 mM Tris HCl pH 8.3
192 mM Glycine	192 mM Glycine
0.1% (w/v) SDS	20% (v/v) Methanol

Table 2.1.15 Sequencing Reagents

Chemical	**Supplier**
10x sequencing buffer	Sigma
Big Dye version 3.1	Sigma

Table 2.1.16 Standards and Ladders

Name	**Volume**	**Purpose**	**Supplier**
1 kb DNA Ladder	6 µl	DNA standard	NEB
Precision Plus Protein Dual colour Standard	5 µl	SDS-PAGE	BioRad

2.2 METHODS

2.2.1 Cell Line preparations.

2.2.1.1 Cell culture

HeLa, Ishikawa, and MFE 319 cells were grown in a complete Dulbecco's modified Eagle's medium (DMEM) growth medium containing 10% Foetal bovine serum (FBS) and 1% penicillin/ streptomycin in a humidified 5% CO_2 incubator at 37^{0}C.

2.2.1.2 Sub-culturing of Cells

Cells were passaged when reaching 70-80% confluency. They were washed with pre-heated phosphate buffer saline (PBS), trypsinized, and incubated at 37^{0}C till the cells became detached, usually after around 5 min of incubation time. The pre-heated complete DMEM medium was added to neutralize the trypsin and the cell suspension was transferred in various ratios into a 10 cm petri-dish according to how it was needed. A typical split ratio includes 1:5, 1:10, and 1:20.

2.2.1.3 Cell Thawing

The cells were thawed quickly at 37^{0}C, 5 ml complete DMEM medium was added, and cells were centrifuged at 900 rpm for 5 min. Afterwards, 10 ml DMEM was added to the cell pellet and transferred to a 10 cm petri-dish plate and placed in the 37^{0}C and 5% CO_2 incubator to grow.

2.2.1.4 Cell Freezing.

After trypsinization, cells were resuspended into a 5 ml pre-heated complete DMEM medium and centrifuged at 900 rpm for 5 min. The supernatant was discarded, and freezing medium (10% FBS, 10%DMSO and 80% DMEM) was added to the pellet and moved into cryovials. The cells were then transferred into a cryovial storage box and placed at –80^{0}C for some time before being transferred into liquid nitrogen for longer storage.

2.2.2 Transfection.

Cells were seeded (1:5 dilution) into a 6-well plate containing 12 mm coverslips and were left overnight to grow to about 70-80% confluency. The medium on the cells was changed to an antibiotic-free DMEM + 10% FBS, and the cells were transfected with 2-µg plasmid using 6 µl Lipofectamine 3000 and 4 µl P3000. The transfection reagent was diluted in optiMEM. Incubation time was 24-48 hours in a humidified 5% CO_2 incubator at 37^{0}C.

2.2.3 Immunostaining and Microscopy.

After transfection, the coverslips were removed and placed into a new 6-well plate for immunostaining and then washed 2x with PBS. The cells were fixed with 3.7% PFA/PBS for 10 min at RT followed by 3x washes with PBS. Afterward, the cells were permeabilized with 0.25% Triton X-100/PBS at RT for 10 min, blocked with a blocking buffer containing 5% goat serum in 0.05% Triton X-100 / PBS for 1 h at RT. The slips were moved to a humid chamber, following an incubation period of 1 h with the primary antibody at RT and, then the slips were incubated with secondary antibody in the dark for 1 h at RT. All antibodies used were diluted in the same blocking buffer. In between incubation with the antibodies, the cells were washed 4x with PBS for 5 min on a shaker.

The coverslips were dipped into water and mounted upside down containing the cells on a glass slide using ProLong™ Glass Antifade Mountant with NucBlue™, the glass slide was then left to incubate for 1 h at RT before transferring to 4^0C until imaging was performed.
The imaging was done using a DMI 6000 B fluorescence microscope from Leica Microsystems and the images were processed using Leica Application Suite X software.

2.2.4 Molecular cloning

Molecular cloning was performed on EGFP-C1-plasmid to insert the NLS sequence from prothymosin α (ProTα) (Rubtsov et al. 1997) and then SKIP. First, EGFP-C1 plasmid was digested at Nhe1 restriction site, followed by an in-fusion cloning of the NLS. And secondly, NLS-EGFP-C1 plasmid was digested at EcoR1 and Bgl11 site, followed by an in-fusion reaction of SKIP. A schematic representation of the final plasmid is shown in the appendix.

2.2.4.1 Digestion

Nhe1 digestion of EGFP-C1 plasmid

EGFP-C1 plasmid was digested in a 20 µl reaction. The reaction contained 5600 ng EGFP-C1 plasmid, NE Buffer 2, 0.2 mg/ml BSA, 30 U Nhe1 enzyme. It was then incubated at 37^0C for 24 h.

EcoR1 and Bgl11 digestion of NLS-EGFP-C1 plasmid.

NLS-EGFP-C1 was digested in a 20 µl reaction. The reaction contained 487.4 ng plasmid, 10 U EcoR1 enzyme, and Cutsmart 3.1 buffer and then incubated at 37^0C for 2 h. After the incubation, 0.2 M NaCl and 5 U Bgl11 enzyme were added to the reaction and then incubated overnight.

2.2.4.2 In-Fusion cloning.

In-Fusion of Nhe1 digested EGFP-C1 plasmid.

An In-fusion reaction was performed to insert the NLS sequence into the digested EGFP-C1 plasmid. The reaction set-up included the following: 69 ng digested plasmid, 52 ng NLS and 2 µl (v/v) 5x In-Fusion enzyme to a total of 10 µl. The reaction was incubated for 15 min at 50^0C and immediately placed on ice to stop the reaction.

In-Fusion of EcoR1 and Bgl11 digested NLS-EGFP-C1 plasmid.

An In-fusion reaction was performed to insert SKIP into the digested NLS-EGFP-C1 plasmid. The reaction set-up includes the following: 68.3 ng SKIP plasmid, 89.3 ng NLS-EGFP-C1 plasmid, and 2 µl (v/v) 5x In-Fusion enzyme to a total of 10 µl. The reaction was incubated for 15 min at 50^0C and immediately placed on ice.

2.2.5 PCR Techniques.

2.2.5.1 Site directed Mutagenesis.

Site directed mutagenesis was done to insert a mutation into K439A-K440L-PTB and NLS-EGFP-SKIP. The PCR reaction set-up included the following: 15 ng DNA template, 0.1 µM forward and reverse primer (*Table 2.1.12, PTB-R437L fwd. & rev primers and EGFPC1-NLS-SKIP-ATG fwd & rev primers*), 0.6 mM dNTP, 2% DMSO, 1 mM $MgCl_2$ and 2 U Phusion DNA polymerase to a final volume of 50 µl. PCR cycling program includes pre-denaturation at 98^0C for 1 min, followed by 25 cycles of denaturation at 98^0C for 10 sec, annealing at 60^0C for 30 sec, extension at 72^0C for 6 min and a final elongation at 72^0C for 7 min. The samples were left for storage at 10^0C until they were taken out of the PCR machine.

2.2.5.2 Colony PCR.

A colony PCR was performed to test for positive clones after transformation. The colonies were picked and placed into a test-tube containing 20 µl 5x FIREPol® Master Mix and 3 µM forward and reverse primers (*Table 2.1.12, EGFPC2 fwd. & rev primers)* to a total volume of 100 µl. The cycling program for reaction includes the following: pre-denaturation 95^0C for 15 min followed by a 35-cycle denaturation at 95^0C for 30 sec, annealing at 57^0C for 30 sec, elongation at 72^0C for 2 min and a final elongation at 72^0C for 7 min and the samples were left for storage at 10^0C until they were taken out from the PCR machine. Afterwards, agarose gel electrophoresis was done to check the positivity of the samples.

2.2.5.3 PCR cloning.

SKIP was subcloned into the EcoR1 sites of NLS-EGFP-C1 using PCR. The reaction was done using the same procedure as the SDM. The primers used were cloning primers (*Table 2.1.12, EGFPC2 fwd. & rev primers)*. The PCR cycling program included a pre-denaturation at 98^0C for 40 sec, followed by a 35-cycle denaturation at 98^0C for 10 sec, annealing at 57^0C for 30 sec, extension at 72^0C for 1.3 min and a final elongation at 72^0C for 7 min. The samples were left for storage at 10^0C until they were taken out of the PCR machine.

2.2.6 Agarose gel electrophoresis.

Agarose gel electrophoresis was used to estimate the size and purity of the DNA fragments from the samples used. The samples were mixed with DNA loading buffer and then run on a 1.2% agarose gel made in TAE buffer and stained with the DNA dye Nancy 520 (1:50000) at 100 V for 40 – 60 min. 2-log DNA ladder was used as a marker for the samples. Images were visualized using BioRad GelDoc™ Imager.

2.2.7 Transformation.

To create large copies of the targeted DNA for subsequent use, the PCR products were transformed into super competent bacterial cells (XL-1 blue). For the purpose of protein expression, plasmids were transformed into BL21-DE3 codon plus bacteria. 4.5 µl PCR products was mixed with 50 µl competent cells (XL-1 blue) or 170 ng DNA was mixed with 5 µl (BL-21DE3). The reaction was placed on ice for 30 min (XL-1 blue)/ 20 min (BL-21) afterward, heat-shocked for 40 sec at 42^0C (XL-1 blue) and 30 sec (BL21-DE3), it was then immediately placed on ice for 2 min. 80 µl SOC medium was added and incubated for 60 min at 37^0C with shaking at 250 rpm. The cells were then plated on LB-agar plates containing the appropriate antibiotics suitable for the plasmid (100 µg/ml ampicillin or 50 µg/ml kanamycin) and then incubated at 37^0C overnight for the bacteria carrying the plasmids to grow.

2.2.8 Plasmid DNA Purification.

For DNA miniprep, 1 – 3 colonies were picked from the bacteria carrying the plasmids and were added to 5 ml LB medium while for DNA maxi/midi prep, 1 colony was picked and added to 100 ml LB medium with the appropriate antibiotics suitable for the plasmid (100 µg/ml ampicillin or 50 µg/ml kanamycin) and left to incubate overnight at 37^0C whilst shaking. The cultures were centrifuged for 10 min at 3250 rpm after which the purification was done. The plasmid gel purification was done using NucleoSpin® Plasmid purification kit from Machery-Nagel. All the procedures were according to the protocol to get the maximum DNA purity.

2.2.9 Measurement of Nucleic acid concentration and purity

DNA concentration and purity was obtained by measuring the absorbance at 260/280 nm using NanoDrop® 1000 Spectrophotometer.

2.2.10 DNA Sequencing.

DNA sequencing was performed using the BigDye v.3.1 protocol. The reaction master-mix was made to a total volume of 10 µl containing 400 ng of the plasmid DNA, 0.2 µM of required primer (*Table 2.1.12, sequencing primers*), 10 % (v/v) sequencing buffer, 10 % (v/v) BigDye 3.1. The PCR cycling program includes pre-denaturation at 96^0C for 10 sec, followed by 30 cycles of denaturation at 96^0C for 10 sec, annealing at 50^0C for 5 sec, elongation at 60^0C for 4 min. The PCR products were allowed to cool down for 7 min at 4^0C and remained at 10^0C until the products were collected. After collection, 10 µl milli-Q was added to each of the products and were then taken to the University of Bergen sequencing facility.

2.2.11 GST-tagged Protein expression and purification

Bacteria colonies were picked from the transformed BL-21DE3 codon plus cell plate were left to grow overnight at 37^0C into 5 mL LB medium containing 100 µg/ml ampicillin. 5 mL of the overnight culture were inoculated into 500 mL LB medium containing 100 µg/ml ampicillin and left to incubate at 37^0C until the OD reached maximum 1. 0.5 mM – 1 mM Isopropyl-B-D-thiogalactopyranoside (IPTG) was then added to the culture afterwards and the culture was left to grow at 18^0C overnight. The culture was centrifuged at 6 000xg at 4^0C for 20 min after which the supernatant was discarded. The pellet was resuspended in 25 ml lysis buffer (PBS pH 7.4, 500mM NaCl, 10 mM KCl, 10 mM $MgCl_2$, 0.5% NP40, 2 mM DTT, 10% glycerol 1 tablet of EDTA free protease inhibitor). The lysate was sonicated 3x for 1 min (10 sec on, 2 sec off with an amplitude of 40%). The sonicated lysate was centrifuged for 40 min at 18 000xg after which the supernatant was added to 1 mL glutathione of Sepharose4B bead and was left to bind overnight on a shaker at RT until the supernatant was removed completely after which a 3-time wash with the washing buffer (PBS pH 7.4, 500 mM NaCl, 10 mM KCl, 10 mM $MgCl_2$, 10% glycerol, 2mM DTT) was done and was allowed to filter. The elution buffer (50 mM tris pH 7.6, 250 mM NaCl, 10 mM KCl, 10 mM $MgCl_2$, 2 mM DTT, 4% glycerol, 20 mM reduced glutathione) was then added to the GST fused recombinant proteins and left to incubate at RT for 30 min after which it was left to elute, and the supernatant was collected. Two elution were performed.

2.2.12 Protein Analysis.

SDS-PAGE and western blot analysis was performed to separate and identify the proteins based on their molecular weight and to assess protein levels.

2.2.12.1 Protein concentration measurements.

Five series of different dilutions of BSA in RIPA buffer were set up in tubes with the following final BSA concentrations (µg/µl): 0.625, 1.25, 2.5, 5, and 7.5. 2 µl of RIPA buffer was pipetted (blank) into 96-well plate alongside the BSA concentrations and the cell lysate all in triplicates. 200 µl BCA (BCA protein assay reagent A+ Reagent B) was added into each well plate, followed by 10 min incubation at 37^0C. After incubation, the absorbance was measured at 562 nm (Abs562) with an EPOCH microplate reader using Gene5 software. The average of the BSA standards concentrations was plotted against the corresponding BSA Abs562 averages in Excel. The concentration of cell lysate was calculated from the average of Abs562 using the Excel equation.

2.2.13 SDS-PAGE

Samples were mixed with 5xSDS sample buffer boiled for 5 min at 95^0C and then loaded into a discontinuous acrylamide gel containing 8% stacking gel and 10% resolving gel. A Running buffer (25 mM Tris HCl pH 8.3, 192 mM Glycine, 0.1% (w/v) SDS) was used and the gel was run at 80 V until the dye reached the end of the stacking gel, and the voltage was increased to 120 until the dye reached the bottom of the resolving gel.

2.2.14 Staining and imaging of the protein gels

For protein expression samples, the gels were stained using Imperial Coomassie protein stain overnight then destained in distilled water. The gels were then imaged using BioRad GelDoc™ Imager.

2.2.15 Western Immunoblotting

The gel was then packed in a sandwich-like manner and transferred into a nitrocellulose membrane with Transfer buffer (25 mM Tris HCl pH 8.3, 192 mM Glycine, 20% (w/v) methanol) at 100 V for 10 min after which the voltage was increased to 120 V for 1 h.

The blot was first blocked-in blocking buffer containing 5% milk in TBS-T and left to incubate overnight at 4^0C on a shaker. After incubation, the blot was rinsed multiple times with 0.05% Tween20/ TBS-T until the milk cleared out, following a 2-hr incubation period with the primary antibody at RT on the shaker and, then an incubation with secondary antibody conjugated with horseradish peroxide (HRP) in the dark for 1 hr. at RT. All antibodies used

were diluted with the blocking buffer containing 5% goat serum in 0.05% Triton X-100 in PBS. In between the incubation with the antibodies, the blot was washed 6x with 0.05% Tween20 in TBS-T, followed by a 3x wash step for 10 minutes on a shaker. The blot was then incubated with SuperSignal™ West Pico PLUS Chemiluminescent Substrate for 5 min and imaged using BioRad GelDoc™ Imager.

3.0 RESULTS

3.1 The GST-PTB R437L-K439A-K440L mutant protein did not express.

Previously, our group has validated the direct interaction of GST-PTB to PPIn [figure 5**A-B**] and has confirmed that the effect of PTB-K439A-K440L mutant on PPIn-binding to GST-RRM3 showed a reduction on all the PPIn-binding lipids [figure 5**E**] and when tested on full-length (FL) PTB, it resulted in a partial reduction binding [figure 5**F**] indicating a possibility of some other PPIn-binding residues. Here, we introduced an additional mutation on the arginine 437 [figure 6**A**] mainly because it is also a basic residue, solvent accessible and it is in proximity with the K439-K440 residues that are involved in the interaction. Our goal gravitated toward the complete removal of PPIn-binding to PTB *in vitro* and so, led us to investigate the effect that an additional mutation has on the interaction.

In order to examine this, SDM was performed on pGEX-PTB-K439A-K440L using the primers listed in *Table 2.1.12* to generate pGEX-PTB-R437L-K439A-K440L. The R437L mutation was confirmed by sequencing. The recombinant GST-FL-PTB WT, K439A-K440L and R437L-K439A-K440L mutant proteins were expressed in BL-21DE3 codon plus bacteria and purified. The expressed and purified proteins were then separated by SDS-PAGE [figure 6**B-C**]. The expressed GST-PTB-WT and K439A-K440L in *figure 6**B*** showed the two thick bands highlighted by the black arrowheads when the bacteria lysates were induced with 0.5 mM IPTG, indicating fairly the expected size of GST-PTB which is 82 k Da (GST – 25 k Da + PTB –57 k Da [Figure 7**B**]). When the same amount of IPTG was used to induce PTB-R437L-K439A-K440L, there was no expression of the protein (result not shown). However, when induced with 1 mM IPTG, a faint band was observed at the expected size (red arrowhead, 6**B**). This observation led to increasing the amount of NaCl used both in the lysis and washing buffer and the addition of glycerol used to lyse the bacteria culture and wash the bound beads during purification. The bacteria were centrifuged, and the pellets were lysed and sonicated. The sonicated lysates were incubated with glutathione of Sepharose4B beads, and the bound proteins were washed and eluted using the column filtration method. The flowthrough obtained after washing and the eluates were resolved by SDS-PAGE and Coomassie-stained. The result observed from the purified proteins [figure 6**C**] showed the presence of both PTB-WT and PTB-K439A-K440L eluates while PTB-R437L-K439A-K440L was absent. With this result, we could not perform a lipid overlay assay to check the effect of PTB-R437L-K439A-K440L on the PPIn binding to PTB.

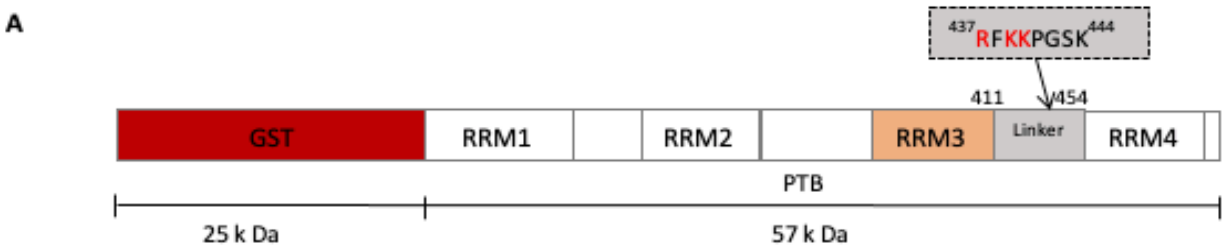
A
437RFKKPGSK444
411
454
GST
RRM1
RRM2
RRM3
Linker
RRM4
PTB
25 k Da
57 k Da

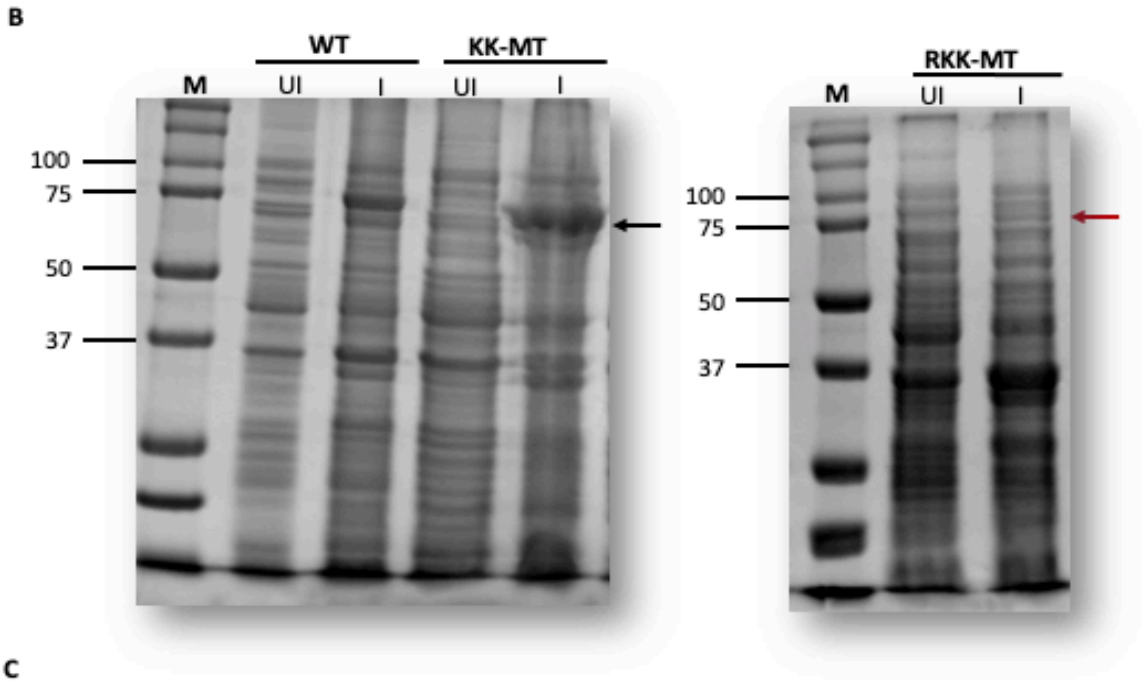
B
WT
KK-MT
RKK-MT
M
UI
I
100
75
50
37

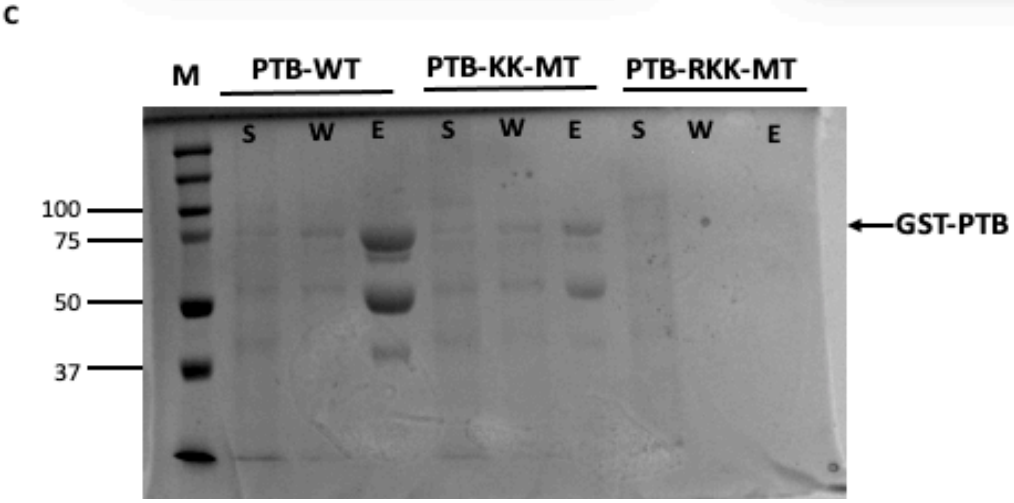
C
M
PTB-WT
PTB-KK-MT
PTB-RKK-MT
S
W
E
100
75
50
37
GST-PTB

Figure 6: Expression and Purification of GST-FL-PTB WT, K439A-K440L, and R437L-K439A-K440L. **(A)**, Schematic representation of GST-fused PTB containing the RNA recognition motifs (RRMs) the linker containing the residues involved in PPIn binding to PTB. The residues K439K440 in red were the mutated residues in previous work while R437 is the additional mutation included in this study. **(B)**, The pGEX-PTB WT (WT), pGEX-PTB-K439A-K440L (KK-MT), and pGEX-PTB-R437L-K439A-K440L (RKK-MT) plasmids were transformed into BL-21DE3 bacteria. Bacteria lysates from un-induced (UI) and induced (I) with 0.5 mM IPTG (WT and KK-MT) or 1 mM IPTG (RKK-MT) were resolved on SDS-PAGE gels and Coomassie-stained. The arrowheads highlight expected bands for expression of the proteins. **(C),** The supernatant **S** obtained from the sonicated lysates when centrifuged were bound to glutathione of Sepharose4B beads, washed **W**, and eluted **E** and were then resolved on SDS-PAGE gels and Coomassie-stained. Arrowheads highlight the expected bands for the purified proteins. **M** represents protein standard in kilo Dalton (k Da)

3.2 Overexpression of PTB-R437L-K439A-K440L mutant has no effect on PTB localisation at the subcellular level.

In order to investigate the localization of PTB following an overexpression of PTB-R437L-K439A-K440L mutant *in vitro*, we generated EGFP-tagged PTB-R437L-K439A-K440L-construct via SDM [figure 7**A**]. The construct was transfected into Ishikawa cells (endometrial cancer cells) alongside EGFP, EGFP-PTB-WT, and EGFP-PTB-K439A-K440L constructs. EGFP was used as control. The cells were labelled with DAPI to visualise the nuclei. The result of the microscopy is shown in *figure 7**B***. The EGFP showed expression of EGFP in the nucleus and a little expression in the cytoplasm. On the other hand, the EGFP-tagged WT, K439A-K440L, and R437L-K439A-K440L mutants highlighted nuclear expression. We observed that the nuclear localization of the tagged R437L-K439A-K440L is quite similar to both WT and PTB-K439A-K440L, if not the same. However, we observed some irregularities in the shape of the nuclei, and we quantified it. The graph of the quantification is shown in *figure 7**C***. The irregularity of cells transfected with PTB-K439A-K440L increased as compared to PTB WT. But not a lot was observed in PTB-R437L-K439A-K440L as compared to PTB-K439A-K440L or WT. In addition, we performed a western blot analysis to assess the protein levels. The bands observed corresponded to the expected size for EGFP (27 k Da) and EGFP-PTB which is 84 k Da (EGFP- 27 k Da + PTB- 57 k Da) [figure 7**C**]. The intensity of the band observed in WT, K439A-K440L, and R437L-K439A-K440L is more or less the same. This indicates that the overexpression of R437L-K439A-K440L-PTB does not have any effect on PTB localisation at the subcellular level.

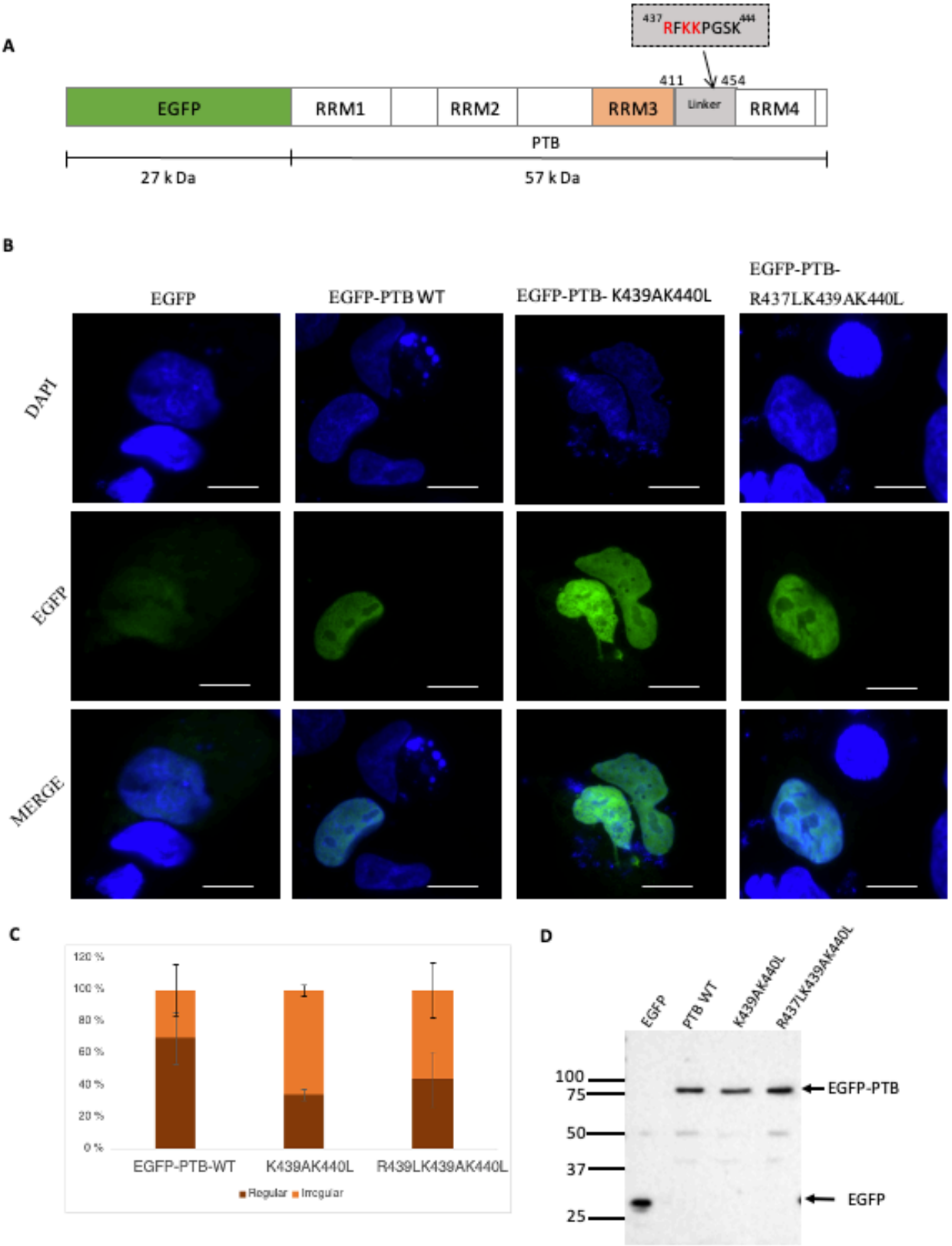
A
437 RFKKPGSK 444
411
454
EGFP
RRM1
RRM2
RRM3
Linker
RRM4
PTB
27 k Da
57 k Da
B
EGFP
EGFP-PTB WT
EGFP-PTB- K439AK440L
EGFP-PTB-
R437LK439AK440L
DAPI
EGFP
MERGE
C
120 %
100 %
80 %
60 %
40 %
20 %
0 %
EGFP-PTB-WT
K439AK440L
R439LK439AK440L
Regular
Irregular
D
EGFP
PTB WT
K439AK440L
R437LK439AK440L
100
75
50
37
25
EGFP-PTB
EGFP

Figure 7: Overexpression of EGFP-PTB-R437L-K439A-K440L mutant does not influence PTB localisation at the subcellular level. (A), Schematic representation of EGFP-tagged PTB containing the RRMs and the linker containing the mutated residues (in red) involved in PPIn binding to PTB. **(B)**, Ishikawa cells were transfected with EGFP as control, EGFP-PTB WT and EGFP-PTB-K439A-K440L and EGFP-PTB- R437L-K439A-K440L constructs for 24 h. The cells were stained with DAPI to detect the nuclei. The images are representative of the dominant localization pattern from 3 experiments. The images were taken using fluorescent microscopy at 100X magnification. The scale bar is 5 μm. **(C)**, Quantification of nuclear shape regularity (brown) and irregularity (orange) observed from the immunostaining images of EGFP-PTB WT and EGFP-PTB-K439A-K440L and EGFP-PTB- R437L-K439A-K440L constructs highlighting the SD. Quantification was done based on two biological experiments and from 28 total number of cells from EGFP-PTB WT, 30 from K439A-K440L and 26 from R437L-K439A-K440L respectively. (**D**), Cells extracted after transfections were subjected to western blotting following a detection of anti-GFP.

3.3 PI3K-p110β inhibition reduces the protein level of PTB in MFE-319 cells.

Although the function of PtdIns (4,5)P_2 is not completely understood in the nucleus, however, it has been found to be associated with a tumour-suppressing protein called p53, a protein that protects the genome against cellular stress, but it is frequently mutated in cancer. PtdIns(4,5)P_2-generating enzyme, PIP5KIα has been demonstrated to regulate p53 stability in the nucleus (Choi et al. 2019). Furthermore, previous studies from our group have shown a molecular association proving that signalling lipids including PtdIns(4,5)P_2 and PtdIns(3,4,5)P_3 are involved in the interaction with PTB (Lewis et al. 2011; Mazloumi Gavgani et al. 2021). Further investigation then reported that the inhibition of PIP5KIα using PIP5KIα inhibitor - ISA2011B decreased protein expression levels of mutated p53 (Choi et al. 2019). Based on this study (Choi et al. 2019), we hypothesized that PtdIns(4,5)P_2 may regulate PTB protein levels.

To investigate this possibility, we manipulated the levels of PtdIns(4,5)P_2 and PtdIns(3,4,5)P_3 by inhibiting PIP5KIα and PI3K-p110β (enzyme that produces PtdIns(3,4,5)P_3 from PtdIns(4,5)P_2) [figure 8**A**]. MFE-319 cells (endometrial cancer cells) were chosen because they express high levels of PTB and exhibit a large number of cells that are PNC positive (unpublished data from previous work from the group). MFE-319 cells were treated with ISA2011B which is a PIP5KIα inhibitor and KIN193 which is a PI3K-p110β inhibitor for 24 h. Cells were treated with DMSO as control. After the treatment, the cells were immuno-stained with antibodies against PTB and PtdIns(4,5)P_2. The result of the immunostaining is shown in *figure 8**B***. The results showed that the control cells exhibited PTB protein levels in the nucleus and in PNC foci as expected while in the treated cells, there is a reduction in the protein levels. Interestingly, in the cells treated with KIN193, the total level of nuclear PTB

greatly decreased compared to control cells. While the reduction observed in cells treated with ISA2011B was not much as compared to control cells. The PTB foci detected in these cells also indicate that the PNC is also detected. PtdIns(4,5)P_2 levels, on the other hand, may have an even expression in the nucleus both in the cells treated with ISA2011B and KIN193, although we expect that there should be a reduction in the expression level in cells treated with ISA2011B. To further analyse PTB levels obtained from immunostaining, we examined the protein expression levels of PTB in cells treated as well as in the control cells using western immunoblotting [figure 8**C**]. Cell extracts were made by collecting the attached and detached cells after treatment and then subject cell extracts to SDS-PAGE to separate the protein before western blot analysis. As a result, we observed a reduction in PTB levels in cells treated with KIN193 compared to control cells when treated with ISA2011B. A confirmation of this is shown when we quantified PTB protein levels was normalized to β-actin [figure 8**D**]. Quantification of results was done using a representative of 3 experiments. These results indicate that PI3K-p110β activity may contribute to regulating PTB levels.

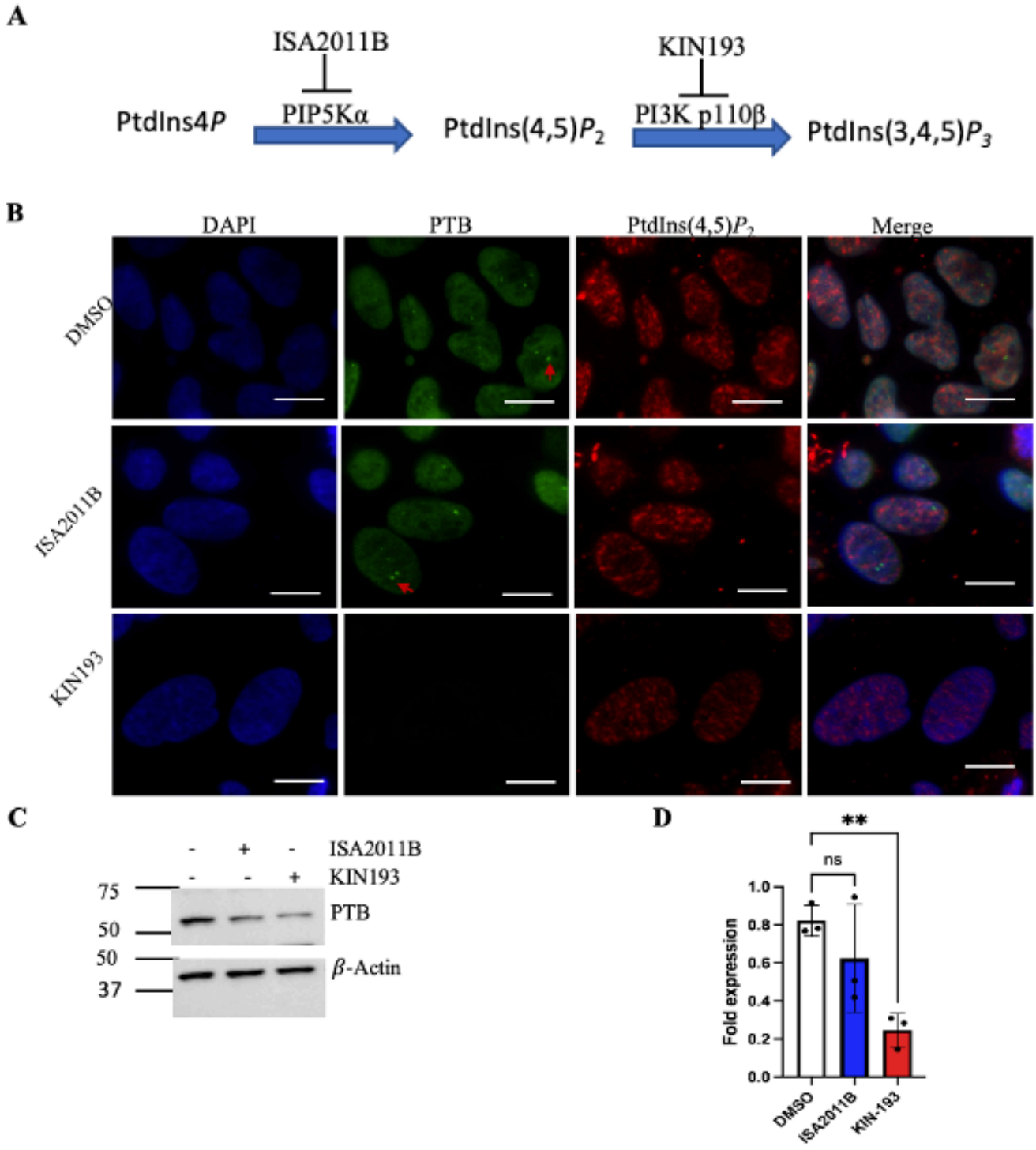

Figure 8: **PI3K-p110β inhibition reduces the protein levels of PTB in MFE-319 cells. (A)** Schematic representation of PtdIns(4,5)P_2 and PtdIns(3,4,5)P_3 metabolism including their metabolizing enzymes (PIP5KIα and PI3K-p110β) and their inhibitors (ISA2011B & KIN193). **(B)** MFE-319 cells were treated with PIP5KIα (ISA2011B) or PI3K-p110β (KIN193) inhibitors for 24 h and were stained with anti-PTB and anti-PtdIns(4,5)P_2. The cells were stained with DAPI to detect the nuclei. The images were taken using fluorescent microscopy at 100X magnification. Arrowheads represent the PTB foci in the nucleus indicating the presence of PNC. The scale bar is 5 µm. Images are representative of 4 experiments. (**C**) Western blot showing PTB levels from the cells treated with either inhibitor. β-actin was used as the loading control while

DMSO was used as treatment control for the inhibitors. **(D)** A fold expression of PTB protein levels against β-actin highlighting the mean ± SD of a representative of 3 experiments. The symbol (**) indicates that the p-value from the t-test performed was $p<0.01$ while ns (not significant) highlights the p-valve from the paired t-test was $p>0.05$. The graph was made using GraphPad Prism 8 software.

3.4 The NLS-EGFP-SKIP fusion protein did not express.

In order to investigate the role of PtdIns(4,5)P_2 in the regulation of PTB levels, we overexpressed a PI 5-phosphatase SKIP, a phosphatase that removes the phosphate group on position 5 on PtdIns(4,5)P_2 and converts it to PtdIns(4)*P*, in the nucleus. SKIP itself is not nuclear and so we fused it to a nuclear localisation signal (NLS) sequence from prothymosin α (Rubtsov et al. 1997). This sequence has been confirmed to target nuclear localization solely to the nucleus excluding nucleoli (Rubtsov et al. 1997). To investigate this, SKIP WT and the SKIP-inactive (PD) were cloned into an NLS-EGFP plasmid to generate NLS-EGFP-SKIP WT and PD constructs [Figure 9**A**]. The constructs were verified by sequencing. MFE-319 cells were transfected with NLS-EGFP, NLS-EGFP-SKIP WT and PD for 24 h. We then examined the expression of GFP in the constructs to check first if EGFP-SKIP is expressed before checking PTB levels. We examined this by separating the cell extracts carrying the constructs via SDS-PAGE and then staining with anti-GFP antibody using western immunoblotting. NLS-EGFP construct was used as control. The result is highlighted in *figure 9**B***. We observed 3 thick bands on the cell extracts carrying the NLS-EGFP construct (27 k Da + 4.1 k Da) following an incubation with anti-GFP which looks quite unusual. NLS-EGFP-SKIP WT and PD were not expressed as there were no bands observed at the expected size (82.1 k Da). These observations were made based on 3 biological experiments. The result indicates that NLS-EGFP-SKIP fusion protein was not expressed in the nucleus and so, we could not proceed with checking PTB levels.

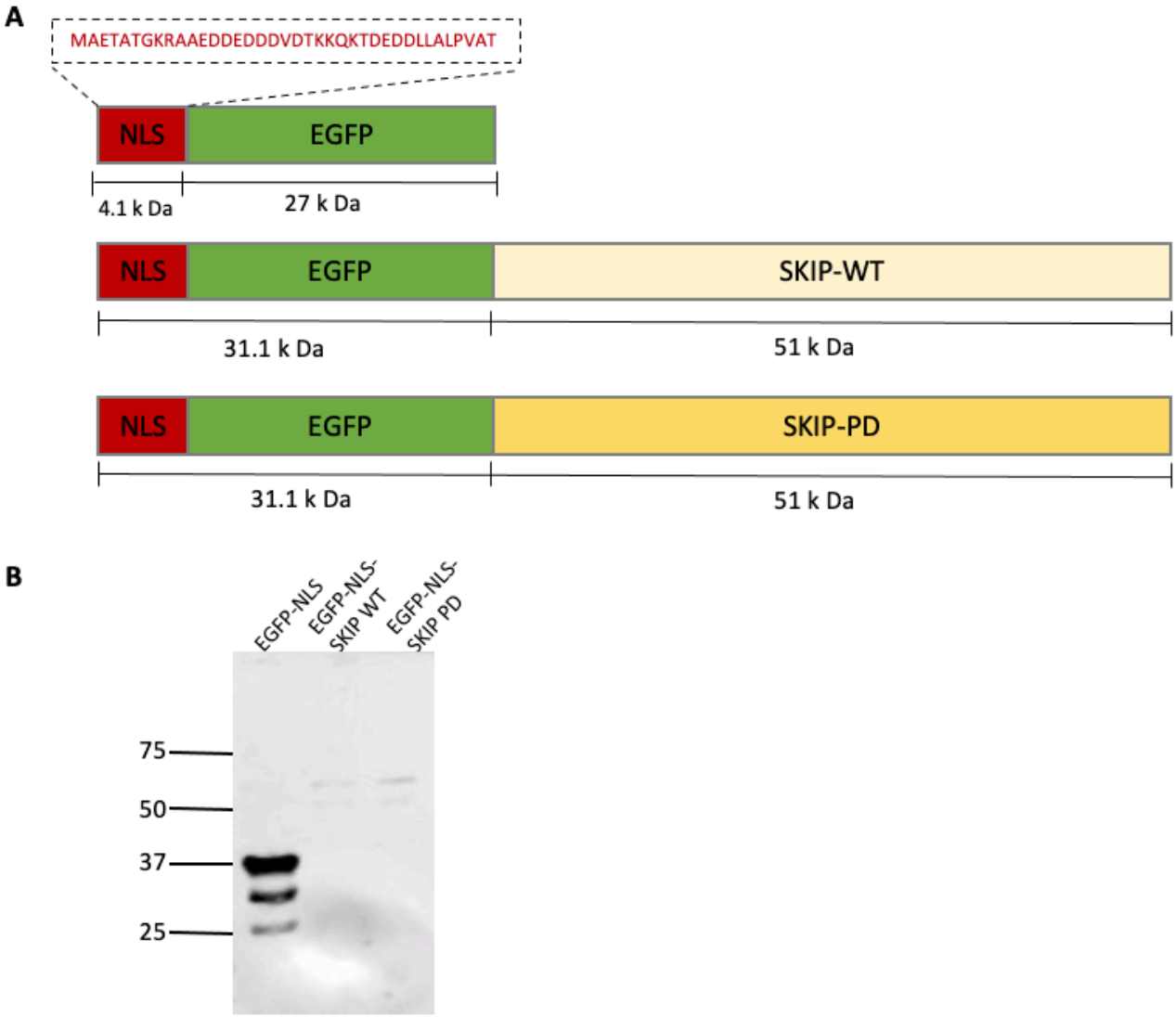

Figure 9: Western immunoblotting of NLS-EGFP-SKIP in MEF-319 cells. (A) Schematic representation of NLS-EGFP, NLS-EGFP-SKIP-WT and NLS-EGFP-SKIP-inactive (PD) constructs. The residues in the box are the NLS and linker residues **(B)** MEF-319 cells were transfected with NLS-EGFP, NLS-EGFP-SKIP WT and NLS-EGFP-SKIP PD for 24 h. The cell extracts collected from the transfection were separated by SDS-PAGE analysed by western blotting and was stained with anti-GFP. NLS-EGFP was used as control. This result is a representative of 3 biological experiments.

4. DISCUSSION

PtdIns(4,5)P_2 has been identified as a nuclear speckles component alongside its metabolizing enzyme and effector proteins where it contributes to pre-mRNA metabolism and splicing (Osborne et al. 2001) while PTB is a splicing factor found in the nucleus that regulates alternative splicing (Garcia-Blanco, Jamison, and Sharp 1989). However, not much evidence has been linked to these two. Interestingly, through a proteomic study, our group has shown a molecular association between PtdIns(4,5)P_2 or PtdIns(3,4,5)P_3 and several splicing factors which PTB is included (Lewis et al. 2011) but its role still remain a mystery.

From results previously obtained by our group, K439 and K440 were shown to partially contribute to PPIn binding to PTB. In the quest of discovering more residues involved in this binding, this study investigated the role of R437 in PPIn-binding properties to PTB. However, we were not able to express the protein and perform a lipid overlay assay. Furthermore, we assessed the localization of EGFP-PTB-R437L-K439A-K440L in Ishikawa cells, but there was no difference in the nuclear localization compared to PTB-WT. In addition, we examined PPIns regulation of PTB protein levels in the nucleus by competitively inhibiting the PtdIns(4,5)P_2 -generating enzyme PIP5KIα and alternatively, inhibiting a PtdIns(3,4,5)P_3-generating enzyme PI3K-p110β that uses PtdIns(4,5)P_2 as a substrate. We found that PIP5KIα inhibitor showed a reduction on PTB protein levels but not significant. However, one interesting result from this thesis was that PI3K-p110β inhibitor showed a huge reduction in PTB protein levels. Also, we overexpressed a 5'phosphatase SKIP, that dephosphorylates PtdIns(4,5)P_2 to PtdIns4P in the nucleus, but we could not express the fusion of NLS-EGFP-SKIP protein.

4.1 R437 does not influence nuclear localisation of PTB.

The potential candidates that may contribute to the remaining PPIn-binding alongside K439 and K440 include arginine 437 and the lysines 428 and 444 [figure 6**C**]. This is because these residues together form a (R-X-KK-X_3-K) motif which is similar to the K/R motif (K/R-(X_{3-7})-K-X-K/R-K/R) that are involved in nuclear PPIn binding proteins (Mazloumi Gavgani et al. 2021; Lewis et al. 2011) and in other lipid-binding proteins (Martin 1998). Additionally, these residues through multiple sequence alignment of PTB and other PTB paralogs in human, have been found to be highly conserved and are close to each other sequence wise (unpublished data from previous work from our group). Furthermore, a study has shown via a structural data analysis that the residues R437 and K444 can be accessible from the surface (Vitali et al. 2006).

This study focused on the residue R437. To check the possibility of its role, SDM was done to generate R437L mutant. However, results obtained from the expression and purification of PTB-R437L-K439A-K440L shows the protein was not expressed [figure 6**B-C**]. Further attempts made to express the protein including manipulating the experiments conditions like temperature, different amount of IPTG remained unsuccessful and so we were not able to perform lipid overlay assay with the protein.

In addition, we overexpressed EGFP-PTB-R437L-K439A-K440L in the nucleus in Ishikawa cells to examine its localisation, the results showed that there was no difference in the localisation as compared to the initial residues that contribute greatly to the binding, EGFP-PTB-K439A-K440L [figure 7**B-D**]. One thing we noted here was that there are some irregularities in the shape of the nuclei in general. The irregularities observed in cells transfected with EGFP-PTB-K439A-K440L increased as compared to EGFP-PTB WT which may also confirm that K439A-K440L mutants affect cell morphology *in vitro* [figure 7**C**]. Although, there are some irregularities observed in cells transfected with EGFP-R437L-K439A-K440L-PTB, but they were just a little bit different from the K439A-K440. We further attempted an overexpression in a different cell line, MFE319, but the expression level was not good for the mutants. Although, we were not able to perform lipid overlay assay and so we cannot conclude from the overexpression experiment, but R437 does not show any difference in the nuclear localisation as compared to K439 and K440.

It will be interesting to know what the next residue in line, K444, would contribute to the binding but right now, an experiment our group is working on is to investigate the effect of the K439 and K440 mutations in addition to mutations in K373, K374 in the FL-PTB. Previously, the results obtained from the RRM3-K373A-K374L mutation showed a reduction in the PPIn-PTB binding in comparison to RRM3-K439A-K440L [Figure 5**E**]. And so, we would like to examine the effect of the FL-PTB-K373A-K374L-K439A-K440L on PPIn-binding to PTB.

Although the role of PPIn binding to PTB is yet to be fully understood, however, it could be that PTB binds to PPIns to regulate its activity or it splices differently when bound to PPIns or maybe not at all and perhaps PPIns themselves, serve as recruiter that locate PTB to the right location for splicing when they temporarily bind to PTB. These are not clear yet, but we hope to get answers when we finally get to remove the PPIn binding to PTB.

4.2 PI3K-p110β activity may contribute to regulating PTB protein levels.

In this study, we discovered that PI3K-p110β activity may regulate PTB protein levels in MFE319 cells. Our results demonstrated that PI3K-p110β inhibitor contributed a huge decrease in the PTB levels [figure 8**C, D**] when MFE319 cells were treated with both PIP5KIα - ISA2011B and PI3K-p110β - KIN193 inhibitors and stained with anti-PTB and anti-PtdIns(4,5)P_2 antibodies [figure 8**B**] and when using western blotting. Based on existing literature (Choi et al. 2019), we hypothesized that PtdIns(4,5)P_2 may regulate PTB levels as the study showed that PIP5KIα and its PtdIns(4,5)P_2 product regulate the stability or function of tumour-suppressor p53 (Choi et al. 2019). However, this hypothesizes was not consistent with the result we obtained from this study. From the immunostaining [figure 8**B**], it was observed that in the cells treated with PIP5KIα-inhibitor, there is indeed a reduction, although not significant, in PTB protein levels but surprisingly, PI3K-p110β inhibitor drastically reduced the protein levels, we confirmed this by the western blot and quantification results [figure 8**C, D**]. The low level of PTB could be due to less stability of the protein or degradation and we do not know if it is a direct effect of PtdIns(4,5)P_2 or PtdIns(3,4,5)P_3. It could be that there is less PtdIns(3,4,5)P_3 upon PI3K-p110b inhibition or high PtdIns(4,5)P_2. But it is unlikely to be due to high level of PtdIns(4,5)P_2 because the results obtained from the inhibition of PIP5KIα did show that there was a reduction in PTB protein levels although not significant. As far as we know, there has just been little report on the effect of PtdIns(3,4,5)P_3 and its metabolizing kinase PI3K-p110β on effector protein stability, thereby indicating results obtained in this study as novel.

The expression levels of PtdIns(4,5)P_2 in our results show an even nuclear staining pattern in the treated cells even though we expect a reduction in the cells treated with PIP5KIα-inhibitor- ISA2011B since it competitively inhibits PIP5KIα that produces PtdIns(4,5)P_2.

4.3 Fusion of NLS-EGFP-SKIP protein was not expressed in the nucleus.

In this study, one of the main goals was to determine the nuclear PPIn that may be involved the regulation of PTB which is a splicing factor. Our method to achieving this was to first manipulate the levels of PtdIns(4,5)P_2 by inhibiting the PPIn kinases (**4.2**) and alternatively, overexpressing a 5'phosphatase SKIP in the nucleus to decrease PtdIns(4,5)P_2 levels. The latter is what we have done here. Our results indicate that the fusion of the protein NLS-EGFP-SKIP did not express in the nucleus [figure 9**B**] following a detection of GFP through western blot to confirm the presence of NLS-EGFP-SKIP in the nucleus. Furthermore, we observed 3

unusual bands in the control construct, NLS-EGFP which could suggest that there is proteolytic degradation or cleavage of the fusion protein. Further attempt to correct the degradation and/or cleavage of the fusion protein include mutation of the start codon ATG in EGFP ORF which could initially allow the DNA polymerase to read both NLS and EGFP as separate sequences. However, the expression pattern of the proteins was the same even after the ATG mutation. And so, checking for PTB levels was not possible.

5 CONCLUSIONS

It is clear that nuclear PPIn function as regulators of splicing and that PTB is a PPIn binding protein. However, the question of which and how PPIn regulate PTB splicing activity is yet to be understood. This study provides evidence that the PI3K-p110β activity may contribute to regulating the protein levels of PTB *in vitro*. This suggests that PTB splicing activity may be regulated by PI3K-p110b activity in the nucleus.

High levels of PTB and the PNC has been reported to be a biomarker and possibly a therapeutic target for cancer (He et al. 2007; Pollock and Huang 2010). In addition, PI3K-p110b level has been reported to be overexpressed in endometrial cancer cell lines (Karlsson et al. 2017) and its activity has been indicated here to be perhaps a regulator of PTB levels. And so, we could potentially target this enzyme to check if it will lead to the reduction of PNC formation and perhaps the PTB-mediated oncogenic properties. Although the mechanism to which PI3K-p110b regulates this activity is not clear yet but we can investigate the stability and/or the degradation of the protein.

6 REFERENCES

Ahn, J. Y., X. Liu, D. Cheng, J. Peng, P. K. Chan, P. A. Wade, and K. Ye. 2005. 'Nucleophosmin/B23, a nuclear PI(3,4,5)P(3) receptor, mediates the antiapoptotic actions of NGF by inhibiting CAD', *Mol Cell*, 18: 435-45.

Babic, I., S. Sharma, and D. L. Black. 2009. 'A role for polypyrimidine tract binding protein in the establishment of focal adhesions', *Mol Cell Biol*, 29: 5564-77.

Cheung, H. C., T. Hai, W. Zhu, K. A. Baggerly, S. Tsavachidis, R. Krahe, and G. J. Cote. 2009. 'Splicing factors PTBP1 and PTBP2 promote proliferation and migration of glioma cell lines', *Brain*, 132: 2277-88.

Choi, S., M. Chen, V. L. Cryns, and R. A. Anderson. 2019. 'A nuclear phosphoinositide kinase complex regulates p53', *Nat Cell Biol*, 21: 462-75.

Darnell, J. E., Jr. 2013. 'Reflections on the history of pre-mRNA processing and highlights of current knowledge: a unified picture', *RNA*, 19: 443-60.

Dickson, E. J., and B. Hille. 2019. 'Understanding phosphoinositides: rare, dynamic, and essential membrane phospholipids', *Biochem J*, 476: 1-23.

Falkenburger, B. H., J. B. Jensen, E. J. Dickson, B. C. Suh, and B. Hille. 2010. 'Phosphoinositides: lipid regulators of membrane proteins', *J Physiol*, 588: 3179-85.

Garcia-Blanco, M. A., S. F. Jamison, and P. A. Sharp. 1989. 'Identification and purification of a 62,000-dalton protein that binds specifically to the polypyrimidine tract of introns', *Genes Dev*, 3: 1874-86.

Hanahan, D., and R. A. Weinberg. 2000. 'The hallmarks of cancer', *Cell*, 100: 57-70.

He, X., M. Pool, K. M. Darcy, S. B. Lim, N. Auersperg, J. S. Coon, and W. T. Beck. 2007. 'Knockdown of polypyrimidine tract-binding protein suppresses ovarian tumor cell growth and invasiveness in vitro', *Oncogene*, 26: 4961-8.

Heo, W. D., T. Inoue, W. S. Park, M. L. Kim, B. O. Park, T. J. Wandless, and T. Meyer. 2006. 'PI(3,4,5)P3 and PI(4,5)P2 lipids target proteins with polybasic clusters to the plasma membrane', *Science*, 314: 1458-61.

Huang, S., T. J. Deerinck, M. H. Ellisman, and D. L. Spector. 1997. 'The dynamic organization of the perinucleolar compartment in the cell nucleus', *J Cell Biol*, 137: 965-74.

Jacobsen, R. G., F. Mazloumi Gavgani, A. J. Edson, M. Goris, A. Altankhuyag, and A. E. Lewis. 2019. 'Polyphosphoinositides in the nucleus: Roadmap of their effectors and mechanisms of interaction', *Adv Biol Regul*, 72: 7-21.

Kamath, R. V., D. J. Leary, and S. Huang. 2001. 'Nucleocytoplasmic shuttling of polypyrimidine tract-binding protein is uncoupled from RNA export', *Mol Biol Cell*, 12: 3808-20.

Karlsson, T., A. Altankhuyag, O. Dobrovolska, D. C. Turcu, and A. E. Lewis. 2016. 'A polybasic motif in ErbB3-binding protein 1 (EBP1) has key functions in nucleolar localization and polyphosphoinositide interaction', *Biochem J*, 473: 2033-47.

Karlsson, T., C. Krakstad, I. L. Tangen, E. A. Hoivik, P. M. Pollock, H. B. Salvesen, and A. E. Lewis. 2017. 'Endometrial cancer cells exhibit high expression of p110beta and its selective inhibition induces variable responses on PI3K signaling, cell survival and proliferation', *Oncotarget*, 8: 3881-94.

Kutateladze, T. G. 2010. 'Translation of the phosphoinositide code by PI effectors', *Nat Chem Biol*, 6: 507-13.

Lemmon, M. A. 2008. 'Membrane recognition by phospholipid-binding domains', *Nat Rev Mol Cell Biol*, 9: 99-111.

Lewis, A. E., L. Sommer, M. O. Arntzen, Y. Strahm, N. A. Morrice, N. Divecha, and C. S. D'Santos. 2011. 'Identification of nuclear phosphatidylinositol 4,5-bisphosphate-interacting proteins by neomycin extraction', *Mol Cell Proteomics*, 10: M110 003376.

Li, B., and T. S. Yen. 2002. 'Characterization of the nuclear export signal of polypyrimidine tract-binding protein', *J Biol Chem*, 277: 10306-14.
Martin, T. F. 1998. 'Phosphoinositide lipids as signaling molecules: common themes for signal transduction, cytoskeletal regulation, and membrane trafficking', *Annu Rev Cell Dev Biol*, 14: 231-64.
Mazloumi Gavgani, F., M. S. Slinning, A. P. Morovicz, V. S. Arnesen, D. C. Turcu, S. Ninzima, C. S. D'Santos, and A. E. Lewis. 2021. 'Nuclear Phosphatidylinositol 3,4,5-Trisphosphate Interactome Uncovers an Enrichment in Nucleolar Proteins', *Mol Cell Proteomics*, 20: 100102.
McCutcheon, I. E., S. J. Hentschel, G. N. Fuller, W. Jin, and G. J. Cote. 2004. 'Expression of the splicing regulator polypyrimidine tract-binding protein in normal and neoplastic brain', *Neuro Oncol*, 6: 9-14.
Osborne, S. L., C. L. Thomas, S. Gschmeissner, and G. Schiavo. 2001. 'Nuclear PtdIns(4,5)P2 assembles in a mitotically regulated particle involved in pre-mRNA splicing', *J Cell Sci*, 114: 2501-11.
Pan, Q., O. Shai, L. J. Lee, B. J. Frey, and B. J. Blencowe. 2008. 'Deep surveying of alternative splicing complexity in the human transcriptome by high-throughput sequencing', *Nat Genet*, 40: 1413-5.
Perez, I., J. G. McAfee, and J. G. Patton. 1997. 'Multiple RRMs contribute to RNA binding specificity and affinity for polypyrimidine tract binding protein', *Biochemistry*, 36: 11881-90.
Pollock, C., and S. Huang. 2009. 'The perinucleolar compartment', *J Cell Biochem*, 107: 189-93.
———. 2010. 'The perinucleolar compartment', *Cold Spring Harb Perspect Biol*, 2: a000679.
Romanelli, M. G., E. Diani, and P. M. Lievens. 2013. 'New insights into functional roles of the polypyrimidine tract-binding protein', *Int J Mol Sci*, 14: 22906-32.
Romanelli, M. G., F. Weighardt, G. Biamonti, S. Riva, and C. Morandi. 1997. 'Sequence determinants for hnRNP I protein nuclear localization', *Exp Cell Res*, 235: 300-4.
Rubtsov, Y. P., A. S. Zolotukhin, I. A. Vorobjev, N. V. Chichkova, N. A. Pavlov, E. M. Karger, A. G. Evstafieva, B. K. Felber, and A. B. Vartapetian. 1997. 'Mutational analysis of human prothymosin alpha reveals a bipartite nuclear localization signal', *FEBS Lett*, 413: 135-41.
Sawicka, K., M. Bushell, K. A. Spriggs, and A. E. Willis. 2008. 'Polypyrimidine-tract-binding protein: a multifunctional RNA-binding protein', *Biochem Soc Trans*, 36: 641-7.
Shah, Z. H., D. R. Jones, L. Sommer, R. Foulger, Y. Bultsma, C. D'Santos, and N. Divecha. 2013. 'Nuclear phosphoinositides and their impact on nuclear functions', *FEBS J*, 280: 6295-310.
Spector, D. L., and A. I. Lamond. 2011. 'Nuclear speckles', *Cold Spring Harb Perspect Biol*, 3.
Stahelin, R. V., J. L. Scott, and C. T. Frick. 2014. 'Cellular and molecular interactions of phosphoinositides and peripheral proteins', *Chem Phys Lipids*, 182: 3-18.
Takahashi, H., J. Nishimura, Y. Kagawa, Y. Kano, Y. Takahashi, X. Wu, M. Hiraki, A. Hamabe, M. Konno, N. Haraguchi, I. Takemasa, T. Mizushima, M. Ishii, K. Mimori, H. Ishii, Y. Doki, M. Mori, and H. Yamamoto. 2015. 'Significance of Polypyrimidine Tract-Binding Protein 1 Expression in Colorectal Cancer', *Mol Cancer Ther*, 14: 1705-16.
Toker, A. 2002. 'Phosphoinositides and signal transduction', *Cell Mol Life Sci*, 59: 761-79.
Vitali, F., A. Henning, F. C. Oberstrass, Y. Hargous, S. D. Auweter, M. Erat, and F. H. Allain. 2006. 'Structure of the two most C-terminal RNA recognition motifs of PTB using segmental isotope labeling', *EMBO J*, 25: 150-62.

Wang, C., J. T. Norton, S. Ghosh, J. Kim, K. Fushimi, J. Y. Wu, M. S. Stack, and S. Huang. 2008. 'Polypyrimidine tract-binding protein (PTB) differentially affects malignancy in a cell line-dependent manner', *J Biol Chem*, 283: 20277-87.

Wang, X., Y. Li, Y. Fan, X. Yu, X. Mao, and F. Jin. 2018. 'PTBP1 promotes the growth of breast cancer cells through the PTEN/Akt pathway and autophagy', *J Cell Physiol*, 233: 8930-39.

Wang, Z. N., D. Liu, B. Yin, W. Y. Ju, H. Z. Qiu, Y. Xiao, Y. J. Chen, X. Z. Peng, and C. M. Lu. 2017. 'High expression of PTBP1 promote invasion of colorectal cancer by alternative splicing of cortactin', *Oncotarget*, 8: 36185-202.

7 APPENDIX

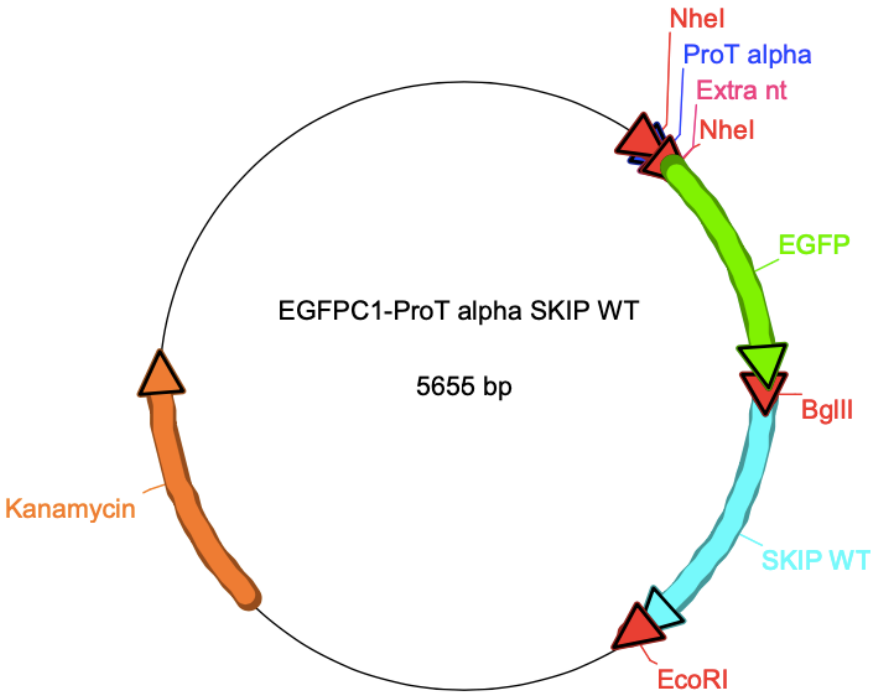

Figure 10: Schematic representation of NLS-ProTα-EGPF-CI-SKIP WT plasmid including the restriction digestion sites (Nhe1, Bgl11 and EcoR1), the antibiotic– kanamycin and the extra nucleotide in frame (Extra nt).